Journal Pre-proofs

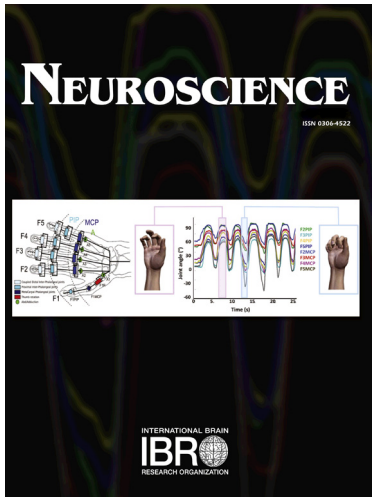

Research Article

Regulation of Alzheimer's disease-associated proteins during the course of epileptogenesis: differential proteomic analysis in a rat model

Eva-Lotta von Rüden, Christina Zellinger, Julia Gedon, Andreas Walker, Vera Bierling, Cornelia A. Deeg, Stefanie M. Hauck, Heidrun Potschka

PII: S0306-4522(19)30612-8
DOI: https://doi.org/10.1016/j.neuroscience.2019.08.037
Reference: NSC 19245

To appear in: *Neuroscience*

Received Date: 13 November 2018
Revised Date: 26 July 2019
Accepted Date: 20 August 2019

Please cite this article as: E-L. von Rüden, C. Zellinger, J. Gedon, A. Walker, V. Bierling, C.A. Deeg, S.M. Hauck, H. Potschka, Regulation of Alzheimer's disease-associated proteins during the course of epileptogenesis: differential proteomic analysis in a rat model, *Neuroscience* (2019), doi: https://doi.org/10.1016/j.neuroscience.2019.08.037

Regulation of Alzheimer's disease-associated proteins during the course of epileptogenesis: differential proteomic analysis in a rat model

Eva-Lotta von Rüden[a], Christina Zellinger[a], Julia Gedon[a], Andreas Walker[a], Vera Bierling[a], Cornelia A. Deeg[b,c], Stefanie M. Hauck[d], and Heidrun Potschka[a, *]

[a]Institute of Pharmacology, Toxicology, and Pharmacy, Ludwig-Maximilians-University (LMU) Munich, Germany

[b]Institute of Animal Physiology, Department of Veterinary Sciences, Ludwig-Maximilians-University (LMU), Munich, Germany

[c]Experimental Ophthalmology, Philipps University of Marburg, Marburg, Germany

[d]Research Unit Protein Science, Helmholtz Center Munich, Neuherberg, Germany

Correspondence: Dr. H. Potschka, Institute of Pharmacology, Toxicology, and Pharmacy, Ludwig-Maximilian-University, Koeninginstr. 16, D-80539 Munich, Germany;
Phone: +49-89-21802662; Fax: +49-89-2180-16556;
E-mail: potschka@pharmtox.vetmed.uni-muenchen.de

Abstract

Clinical evidence and pathological studies suggest a bidirectional link between temporal lobe epilepsy and Alzheimer's disease. Data analysis from omic studies offers an excellent opportunity to identify the overlap in molecular alterations between the two pathologies.

We have subjected proteomic data sets from a rat model of epileptogenesis to a bioinformatics analysis focused on proteins functionally linked with Alzheimer's disease. The data sets have been obtained for hippocampus and parahippocampal cortex samples collected during the course of epileptogenesis.

Our study confirmed a relevant dysregulation of proteins linked with Alzheimer pathogenesis. When comparing the two brain areas, a more prominent regulation was evident in parahippocampal cortex samples as compared to the hippocampus. Dysregulated protein

groups comprised those affecting mitochondrial function and calcium homeostasis. Differentially expressed mitochondrial proteins included proteins of the mitochondrial complexes I, III, IV, and V as well as of the accessory subunit of complex I.

The analysis also revealed a regulation of the microtubule associated protein Tau in parahippocampal cortex tissue during the latency phase. This was further confirmed by immunohistochemistry.

Moreover, we demonstrated a complex epileptogenesis-associated dysregulation of proteins involved in amyloid β processing and its regulation. Among others, the amyloid precursor protein and the α-secretase alpha disintegrin metalloproteinase 17 were included.

Our analysis revealed a relevant regulation of key proteins known to be associated with Alzheimer's disease pathogenesis. The analysis provides a comprehensive overview of shared molecular alterations characterizing epilepsy development and manifestation as well as Alzheimer's disease development and progression.

Keywords

amyloid beta; mitochondrial dysfunction; Adam17; ApoE; status epilepticus; calcium hypothesis

Graphical Abstract

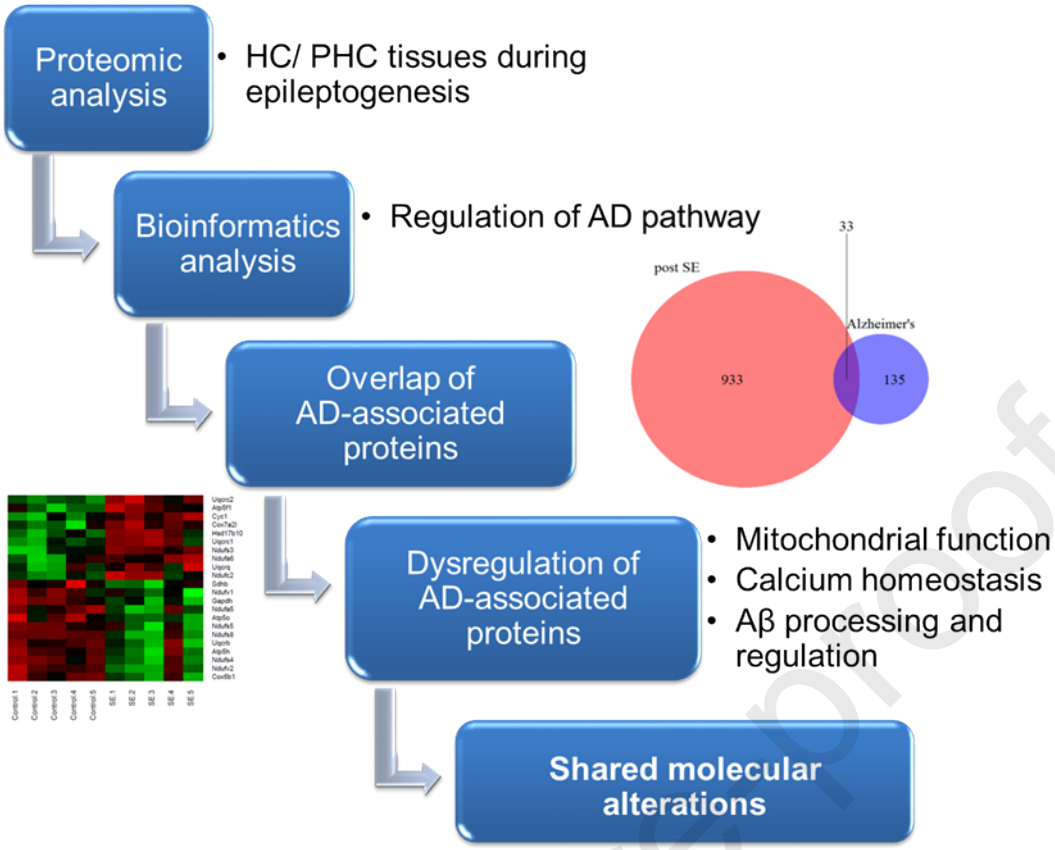

Abbreviations

Alpha disintegrin metalloproteinase – Adam

Alzheimer's disease – AD

Amyloid beta – Aβ

Amyloid precursor protein – App

Apolipoprotein E – ApoE

Calcium-binding regulatory protein calmodulin 1 - Calm1

dpSE – days post SE

Fold change – FC

Hippocampus – HC

Lipoprotein receptor-related protein 1 - Lrp1

Protein phosphatase 3 - Ppp3

Snca - α-synuclein

Status epilepticus – SE

Mapt - microtubule-associated protein Tau, in short: Tau

Temporal lobe epilepsy – TLE

wpSE – weeks post SE

Introduction

Clinical evidence points to a bidirectional link between temporal lobe epilepsy (TLE) and Alzheimer's disease (AD). On one hand, patients with TLE seem to have an increased risk to develop symptoms of an AD-like dementia as well as respective pathological alterations (Noebels, 2011, Kandratavicius et al., 2013, Tai et al., 2016). On the other hand, an increased incidence of seizures has been reported in AD patient subgroups, e.g. in patients with early onset dementia (Larner, 2010, Noebels, 2011, Nicastro et al., 2016, Rauramaa et al., 2018). However, clear-cut conclusions about a functional link between pathologies are difficult to draw from clinical data also taking into account that the symptoms of both diseases might superimpose each other.

From a neuropathological point of view, TLE and AD differently localize in the entorhinal cortex. TLE is classically associated with damage to the medial entorhinal cortex (Du et al., 1995) and, instead, AD involves the lateral entorhinal cortex, both with a superficial localization (Xu et al., 2015). Additionally, third layer cells of the medial entorhinal cortex are more involved in TLE (de Guzman et al., 2008) whereas the second layer is more selectively damaged in AD (Scharfman and Chao, 2013).

Experimental data comparing AD and TLE models confirmed shared cellular and network alterations in the hippocampus (HC) including axon remodeling such as sprouting of mossy fibers, loss of calbindin and transient increases in neurogenesis (de Lanerolle et al., 1989, Jin et al., 2004, Sutula and Dudek, 2007, Gan et al., 2008, Parent and Murphy, 2008, Minkeviciene et al., 2009, Palop and Mucke, 2009, Noebels, 2011). Moreover, it has been reported that seizures can affect cleavage of the amyloid precursor protein (App) and trigger an activity-dependent amyloid beta (Aβ) release from synapses (Cirrito et al., 2005, Lesné et al., 2005, Cirrito et al., 2008, Reyes-Marin and Nuñez, 2017). Furthermore, there is evidence that status epilepticus can introduce amyloid beta deposition in the hippocampus (Baldelli et al., 2010). Pathological investigations in TLE patient tissue also gave first evidence that AD-

like pathological alterations including changes in microtubule-associated protein Tau (mapt, in the following: Tau) expression can occur in subgroups of patients (Kandratavicius et al., 2013, Tai et al., 2016). Functional implications of respective alterations have been suggested by genetic targeting of Tau in AD models as well as in mouse and Drosophila genetic models of epilepsy resulting in a decrease in network hyperexcitability (Zumkehr et al., Noble et al., 2005, Holth et al., 2013, Gheyara et al., 2014, Schoch et al., 2016). However, these effect seem to be gene specific as Tau deletion in two epilepsy models of sodium channel epilepsy, namely Dravet syndrome and Early Infantile Epileptic Encephalopathy, had neither an effect on early mortality rates nor on behavioral seizure activity (Chen et al., 2018).

Considering the current state of knowledge it seems to be of particular interest to analyze the common and shared pathophysiological mechanisms in detail. So far, there is only limited information available about the impact of epileptogenesis and epilepsy on the expression pattern of molecules known to be affected in AD or to be involved in AD development and progression. Therefore, we have performed a large-scale differential proteome analysis in an electrical rat TLE model with spontaneous recurrent seizures and have compared these data sets with available information about differential protein expression in AD and its models. Hippocampal and parahippocampal cortex tissues were sampled at three time points following an electrically-induced status epilepticus (SE) reflecting the early insult phase, the latency phase, and the chronic phase with spontaneous recurrent seizures.

The samples were subjected to proteomics profiling based on a label-free liquid chromatography tandem mass spectrometry (LC-MS/MS) approach. The bioinformatics analysis of the data sets obtained was focused on expression patterns of proteins functionally associated with AD. In previous studies, we have completed a bioinformatics analysis focused on cell stress, extracellular matrix and angiogenesis (Keck et al., 2018) and a co-regulated proteins (Keck et al., 2017). These studies already pointed to the overlap in protein clusters regulated during epileptogenesis with those regulated in neurodegenerative diseases including AD. The latter finding triggered our interest to identify and study AD-associated proteins in our data sets.

The findings provide comprehensive information about the time course of epileptogenesis-associated alterations in expression patterns of proteins functionally linked with AD pathophysiology.

Experimental procedures

Animals and experimental design

Female Sprague Dawley rats (n= 59, 200-224 g; corresponding to an age range of 10–11 weeks) were ordered from Harlan Laboratories (now Envigo; Udine, Italy) and were housed under controlled environmental conditions (22–24 °C, 45–65% humidity, 12 h dark/light cycle) with unrestricted access to tap water and food (Ssniff R/M Haltung Spezialdiäten GmbH, Soest, Germany). Please note that we used female rats based on our characterization of the model (Brandt et al., 2003), which revealed a high mortality rate in male rats. Rats were housed individually (macrolon cages type III; embedding: birk wood granulates, Lignocel® Select Altromin GmbH, Lage, Germany) and received nesting material (Nestlets, Ancare, Bellmore, NY, USA).

The experiments were performed in accordance with the European Communities Council Directive 2010/63/EU, the German Animal Welfare act and were approved by the Government of Upper Bavaria (license number: 55.2-1-54-2532-94-11). Procedures and reporting comply with the ARRIVE guidelines. All efforts were made to minimize pain and discomfort and to reduce the number of animals used in the investigations.

Supplementary Figure 1 (in the appendix at the end of the manuscript) presents the experimental timeline as described in Walker et al. (2016). In short: A combined recording and stimulation electrode was stereotactically implanted into the right basolateral amygdala of all animals according to the brain atlas of Paxinos and Watson (1998) (AP -3.3, LL 4.7 and DV -8.8 mm in relation to bregma) under anesthesia and analgesia (chloralhydrate 360 mg/kg i.p., bupivacaine 0.5% s.c. (Bupivacaine 0.5%, Jenapharm, Jena, German) and meloxicam 1 mg/kg s.c. 30 min pre- and 24 h post-surgery (Metacam, Boehringer-Ingelheim, Ingelheim, Germany)). In addition, animals received pre- and post-surgery (one day before until day seven post-surgery) marbofloxacin 1 mg/kg s.c. (Marbocyl FD 1%, Vétoquinol, Ravensburg, Germany). Six weeks later, a self-sustained SE was induced by continuous electrical stimulation for 25 min with an intratrain pulse frequency of 50 Hz, 700 µA peak pulse intensity and 100 ms trains of 1 ms alternating positive and negative square-wave-pulses at a frequency of 2 Hz. The SE was confirmed by EEG-recordings and terminated after 4 h by diazepam injections (Diazepam-Ratiopharm, Ratiopharm, Ulm, Germany; 20 mg/kg, i.p.). Additional EEG-recordings after diazepam injections confirmed the termination of seizure activity. All animals were continuously observed in glass cages by trained experimenters and according to Racine (1972) seizure severity was scaled and the type of SE was further divided into three different types (Brandt et al., 2003). Only animals exhibiting a generalized convulsive type three SE were used for further analysis. Two days, ten days and eight weeks post SE (dpSE, wpSE; referring to the acute, latency and chronic phase of epilepsy) five

animals per time point and group were randomly chosen and sacrificed by pentobarbital injections (500 mg/kg i.p.; Narkodorm, cp-Pharma, Burgdorf, Germany) and brains were sampled for mass spectrometric analysis. Rats from the chronic phase underwent 19 days of continuous video- and EEG-monitoring (24 h per day, 7 days per week) as described earlier (Russmann et al., 2016, Walker et al., 2016). Corresponding electrode-implanted control animals were subjected to all handling and experimental procedures except for electrical stimulation.

Tissue preparation, mass spectrometry, label-free quantification and protein identification

As described by Walker et al. (2016) the HC and the parahippocampal cortex (PHC) were dissected on ice by an experimenter unaware of group assignment. The tissues were enzymatically digested in 0.05% trypsin/EDTA and mechanically dissociated as described by Uhl et al. (2014). 10 µg total protein per sample were proteolysed with trypsin (Wisniewski et al., 2009) and LC-MS/MS analysis was performed on an LTQ OrbitrapXL (Thermo Fisher Pierce) as described previously (Merl et al., 2012, Walker et al., 2016). All experimenters performing tissue preparation and mass spectrometry were unaware of the treatment groups to exclude any expectation triggered bias.

Label-free quantification was performed with the Progenesis LC–MS software (Version 2.5, Nonlinear Dynamics) as described before (Walker et al., 2016).

MS/MS spectra were exported as Mascot generic files (mgf) and searched with Mascot (version 2.4) using the Ensembl Rat protein database (release 69, 32,971 sequences) for peptide identification with 10 ppm peptide mass tolerance, 0.6 Da fragment mass tolerance and one missed cleavage. Carbamidomethylation was set as fixed modification. Variable modifications were methionine oxidation and deamidation of asparagine and glutamine.

Functional annotation analysis

Before bioinformatics analysis, the corresponding gene symbol was identified as described by Walker et al. (2016) for every quantified protein. The resulting gene lists for each time point and tissue type were used for functional annotation analysis which was performed with the publically available tool Database for Annotation, Visualization and Integrated Discovery (DAVID) v6.7. “Homo sapiens” was selected as list and background species.

In the resulting pathway lists (threshold: a minimum of two protein members and p-value < 0.05) we searched for the enriched AD-pathway.

Identification and expression analysis of AD-associated proteins during the time course of epileptogenesis

AD-associated reference proteins, in total 168, were identified by Kyoto Encyclopedia of Genes and Genomes (KEGG) database (Kanehisa and Goto, 2000, Kanehisa et al., 2016, Kanehisa et al., 2017).

Among all differentially expressed proteins of the HC and PHC at all three analyzed time points we searched for AD-associated reference proteins in our data set resulting in one protein list of AD-associated proteins. This list was used for further analysis.

To identify the amount of AD-associated proteins of both analyzed tissues, the overlap of the AD-reference proteins and the differentially expressed proteins was determined during epileptogenesis and visualized in Venn diagrams.

In the following, we assigned the identified proteins functionally associated with AD into protein groups according to their function: mitochondrial proteins, proteins associated with calcium signaling, proteins associated with Tau, associated with Aβ processing, deposition, plaque formation, and Aβ-associated pathology and analyzed their expression pattern.

For the expression analysis we considered either all quantified (proteins associated with calcium signaling Tau-associated proteins, Aβ-associated proteins, cell death or other cellular processes) or all differentially expressed proteins (mitochondrial proteins). When all quantified proteins were used for the analysis, differentially expressed proteins have been highlighted with an asterisk. Detailed information about the individual FC is given in the cell notes and/or in the **Supplementary Table 1 and 2** (in the appendix at the end of the manuscript).

For the analysis of the mitochondrial protein expression patterns (**Figure 2 A**) of the HC and the PHC proteins quantified at all three time points were considered and the FCs were determined.

Immunohistochemistry

Data obtained by large scale proteomic analysis were further validated by immunohistochemical analysis of selected proteins (Tau and ApoE).

Five animals per time point (two dpSE, ten dpSE and eight wpSE) were deeply anesthetized with pentobarbital (500 mg/kg i.p.; Narkodorm®, cp-Pharma, Burgdorf, Germany) and transcardially perfused with 0.01 M phosphate buffer (pH 7.4). Brains were stored at 4°C in 30% sucrose. Fourty µm coronal sections were obtained, transferred to a cryoprotecting solution and stored at -80°C until further use.

For Tau immunohistochemistry, sections were washed in tris-buffered saline (TBS, pH 7.6) containing 0.05% Tween 20 (Sigma, Taufkirchen Germany) and incubated in sodium citrate (pH 6, 85°C, 30 min) for heat-induced antigen retrieval. Brain slices were washed in TBS/0.005% Tween 20 and transferred into 3% TBS buffered H_2O_2 for 15 min. Sections were incubated with 0.25% casein (Sigma, Taufkirchen, Germany) in TBS for 10 min thereby blocking unspecific protein binding and were then kept overnight in unconjugated rabbit polyclonal anti-Tau antibody (1:3000 in TBS containing 0.25 % casein and 0.1 % Tween 20 at 4°C; ab101854, Abcam, Cambridge, UK). On the following day, sections were rinsed and incubated in secondary biotinylated goat anti-rabbit antibody (1:500 in in TBS containing 0.25 % casein and 0.1 % Tween 20, 30 min, room temperature; 111-065-003 Jackson/Dianova, Hamburg, Germany). Sections were then incubated for 30 min in Streptavidin/HRP at room temperature (1:4000 in TBS, Jackson/Dianova, Hamburg, Germany). Specific antibody binding was visualized by a nickel enhanced DAB reaction. Following blocking with bovine serum albumin and donkey serum in TBS, sections were incubated overnight at 4°C with an anti-NeuN antibody (1:500 in TBS containing Triton X100 and bovine serum albumin; mab377, Millipore, Darmstadt, Germany). Sections were then incubated sequentially with the secondary biotinylated donkey anti-mouse antibody (1:500 in TBS containing donkey serum and bovine serum albumin, 30 min, room temperature; 715-065-151 Jackson/Dianova, Hamburg, Germany), Streptavidin/AP (1:600 in TBS, 45 min, Jackson/Dianova, Hamburg, Germany), and neufuchsin for 20 min. The reaction was stopped by washing in double distilled water. After washing with TBS/0.05% Tween 20, sections were air dried overnight and coverslipped with Entellan.

For ApoE immunohistochemistry, sections were rinsed three times in TBS and afterwards incubated for 30 min in sodium citrate buffer (pH 9) at 80 °C for antigen retrieval. After additional washing in TBS, unspecific binding sites were blocked by 30 min incubation in a blocking solution containing 1% BSA, 1% donkey serum and 0.3% Triton. For immunolabeling of ApoE, we used a polyclonal rabbit antibody (1:1000, AB20874; Abcam, Cambridge, United Kingdom) overnight at 4 °C. Sections were then washed with TBS containing 0.05 % Tween20 and incubated with a biotinylated donkey anti-rabbit antibody (1:1000; 711-065-152; Dianova GmbH, Hamburg, Germany) for one hour at room temperature. Sections were rinsed and incubated for 60 min in horseradish peroxidase-labeled Sreptavidin (1:1400, Dianova GmbH, Hamburg, Germany). To visualize the staining, a nickel-intensified diaminobenzidine reaction was performed. Finally, sections were washed,

mounted onto glass slides, air-dried, dehydrated, and cover-slipped with Entellan (Merck, Darmstadt, Germany).

An experimenter not aware of the treatment conditions performed the unbiased stereological cell counting of Tau- and NeuN-positive cells using the optical fractionator method. The evaluation was performed with the computer-assisted imaging system StereoInvestigator 7.0 (Microbrightfield Europe, Magdeburg, Germany). The hardware consisted of a Leica DMLB microscope (Leica, Bensheim, Germany), a Plan-Neofluar lens (Leica, Bensheim, Germany), a single chip charge coupled device (CCD) color camera (CX9000, Microbrightfield Europe, Magdeburg, Germany), and an AMD Athlon (tm) 64 Processor. The PHC (entorhinal cortex, posterior piriform cortex and perirhinal cortex) of animals with SE and of time-matched electrode-implanted control animals was analyzed in the rostro-caudal dimension from -3.36 mm to -7.44 mm relative to bregma corresponding to the dissected area for mass spectrometry analysis. The area was traced and counting frames were placed automatically and randomly along the area. Tau- and NeuN-positive cells within the counting frame and coming into focus were counted.

Evaluation of ApoE immunohistochemistry was based on labeled area and optical density using a computer image analysis system and performed by an experimenter unaware of group assignment. The hardware consisted of an Olympus BH2 microscope with a Plan-Neofluar objective (Zeiss, Göttingen, Germany), a CCD color camera (Axiocam; Zeiss, Göttingen, Germany), and an AMD Athlon™ 64 processor-based computer with an image capture interface card (Axiocam MR Interface Rev.A; Zeiss, Göttingen, Germany). We used the image analysis software KS400 (Windows Release 3.0; Carl Zeiss Vision, Halbergmoos Germany). The methodology is based on Volk et al. (2004). Prior to image analysis, spatial calibration was performed and a signal threshold was set to exclude background signal for each region analyzed (CA1, CA3 and PHC at Bregma -2.56, -3.14 and -5.8). Consecutively, the obtained data provides information about the ApoE positive labeled area and optical density above the threshold level. Representative images of ApoE immunohistochemistry were captured with a Leica DMLB microscope (Leica Microsystems GmbH, Wetzlar, Germany), an Intel® Core™ i7-4790 @3.60 GHz on 8 cores processor with a NVIDIA GeForce GTX 760 video card and Stereo Investigator software (version 2017.01.1 (64-bit)).

Statistics

As described in detail by Walker et al. (2016), we computed a Mascot-integrated decoy database search, based on the Percolator algorithm, with an average peptide false discovery rate below 2% with a Percolator score cut-off of 13 and a significance threshold of $p < 0.05$. Thus, before computing any further statistics, a FDR adjustment, based on the Percolator algorithm, was performed on the raw data to exclude false positive protein findings.

Identified peptides were re-imported into Progenesis LC–MS and for quantification of unique peptides, a cumulative normalized abundance was calculated by summing the abundances of all peptides allocated to the respective protein. For the further analysis, we considered only proteins with a minimum of two quantified peptides and a confidence score of > 30.

The normalized abundances of the individual proteins were compared with Student's t-test to determine differential abundances of proteins between control and animals post SE. We considered a protein differentially expressed with a p-value (ANOVA) < 0.05. These p-values are given for regulated proteins of the AD pathway in Tables 1 and 2.

We computed individual fold changes (FC) for control and animals post SE by dividing the protein abundance by the mean abundance of the respective control group. Data was organized in a matrix format and zeros were replaced by 1E-20. In the following, data were normalized by log2 transformation according to Key (2012) (FC = log2 (mean animals post SE / mean control animals).

Heat map analysis was performed with R-software x64 3.2.3 and "g-plots"-package heatmap.2 function (Warnes et al., 2015). Protein profiles (rows) were clustered by agglomerative clustering with complete linkage measure.

Immunohistochemical quantifications were statistically analyzed (GraphPrism version 5) by the Student's t-Test with or without Welch's correction, one way ANOVA of variance followed by Bonferroni's multiple comparison test and a p-value < 0.05 was considered significant.

Results

In samples from all time points the bioinformatics analyses revealed an over-representation of proteins functionally associated with AD pathophysiology among the differentially expressed proteins (HC: two dpSE $p < 0.001$; PHC: two dpSE $p = 0.013$, ten dpSE $p < 0.0000001$ and eight wpSE $p < 0.00001$). **Figure 1 A** illustrates the AD pathway with its regulated key proteins, which showed strong enrichment ten dpSE in the PHC. Regulated key proteins as indicated by DAVID are: CxI, CxII, CxIII, CxIV, CxV, ABAD, ADAM17, APP-B1, GAPD, Gq, PLC, CaM, Cn, IP3R and Tau. Thus, referring to a pronounced regulation of

mitochondrial proteins, proteins associated with Aβ processing, deposition and plaque formation, the regulation of the microtubule-associated protein Tau and the regulation of proteins associated with calcium signaling. For detailed information about all regulated proteins functionally linked with AD during the time course of epileptogenesis in hippocampal and parahippocampal cortex tissues see **Tables 1 and 2**.

In total, we identified 63 proteins functionally associated with AD, which proved to be regulated at least once during the course of epileptogenesis in at least one of the brain regions of interest (two dpSE, ten dpSE and eight wpSE). The overlap of regulated proteins from our HC and PHC data sets functionally linked with AD and of the AD-associated reference proteins amounted to 17, 20, and 16 % two dpSE, ten dpSE and eight wpSE, respectively (see **Figure 1 B-D**). The strongest overlap with 33 regulated proteins was evident in the latency phase.

We grouped the 63 identified proteins according to their function into five main groups: mitochondrial proteins, proteins associated with calcium signaling, proteins associated with Tau, associated with Aβ processing, deposition, plaque formation, and Aβ-associated pathology. These functional protein groups were selected, as they are involved in the pathophysiology of AD as well as of epilepsy and epileptogenesis. We described Proteomic alterations in these protein groups in detail further below.

Regulation of mitochondrial proteins

The analysis of our data set revealed a prominent epileptogenesis-associated dysregulation of mitochondrial expression patterns in the PHC and a less pronounced dysregulation in the HC (**Figure 2 A-G** and **Supplementary Tables 1 and 2**). In the PHC and HC 39 and 38 proteins were identified, respectively, which were associated with mitochondrial function. Among these, 22 and 17 PHC proteins and 20 and 18 HC proteins were up- or down-regulated, respectively.

When we analyzed the expression pattern of differentially expressed mitochondrial proteins in detail, several PHC proteins associated with NADH dehydrogenase/ubiquinone regulation and function exhibited a downregulation ten dpSE. These proteins included NADH Dehydrogenase (Ubiquinone) iron sulfur protein 4 (Ndufs4), NADH Dehydrogenase (Ubiquinone) iron sulfur protein 5 (Ndufs5), NADH Dehydrogenase (Ubiquinone) iron sulfur protein 8 (Ndufs8), NADH Dehydrogenase (Ubiquinone) Flavoprotein 1 (Ndufv1), NADH Dehydrogenase (Ubiquinone) Flavoprotein 2 (Ndufv2), and NADH Dehydrogenase (Ubiquinone) 1 Alpha (Ndufa5; see **Figure 1 F** and **Supplementary Table 2**). All these

proteins functionally belong to the mitochondrial complex I or to the accessory subunit of complex 1.

An analysis of this protein subcategory in PHC samples from the early post-insult phase indicated an early induction of NADH Dehydrogenase (Ubiquinone) 1 Beta (Ndufb4), NADH dehydrogenase/ubiquinone 1 alpha subcomplex 6 (Ndufa6) and NADH Dehydrogenase (Ubiquinone) iron sulfur protein 7 (Ndufs7; see **Figure 1 E** and **Supplementary Table 2**). In HC samples, the dysregulation of this subcategory of proteins was less pronounced with changes in the expression rates limited to the early post-insult phase (see **Figure 1 C** and **Supplementary Table 1)**. Here, an early dysregulation of proteins from the accessory subunit of complex 1 was evident with NADH dehydrogenase (ubiquinone) 1 beta subcomplex 5 (Ndufb5), NADH dehydrogenase (ubiquinone) 1 beta subcomplex 7 (Ndufb7), and NADH dehydrogenase (ubiquinone) 1 beta subcomplex 8 (Ndufb8) being up-regulated, and NADH Dehydrogenase (Ubiquinone) 1 Alpha Subcomplex 6 (Ndufa6) being down-regulated.

Cytochrome C oxidase subunit proteins (mitochondrial complex III and IV) were also regulated during the course of epileptogenesis. An early increase in expression levels of Cytochrome C-1 (Cyc1) and of ubiquinol-cytochrome c reductase core protein II (Uqcr2) was determined in the HC and PHC (**Figure 1 E and F** and **Supplementary Table 1** and **2**). These proteins still exhibited altered expression levels during the latency phase and Uqcrc2 remained at increased levels during the chronic phase in the PHC (**Figure 1 F, G** and **Supplementary Table 2**). Moreover, ubiquinol-cytochrome c reductase core protein I (Uqcrc1) and ubiquinol-cytochrome c reductase, complex III subunit VII (Uqcrq) displayed elevated expression levels during the latency phase and still exhibited induced levels in the chronic phase. Ubiquinol-cytochrome c reductase hinge protein (Uqcrh) proved to be up-regulated in the chronic phase as well. Thus, altered expression levels of complex III proteins indicated a pronounced dysregulation of this mitochondrial protein complex in the PHC during the late phases of epileptogenesis.

Both, cytochrome c oxidase subunit Vib polypeptide 1 (Cox6b1) and Cytochrome c oxidase subunit 7A-related protein (Cox7a2l) showed reduced expression rates in the PHC in the latency phase (**Figure 1 F** and **Supplementary Table 2**). During the early post-insult phase, cytochrome c oxidase subunit VIa polypeptide 1 (Cox6a1), cytochrome c oxidase subunit Vic (Cox6c) and cytochrome c oxidase subunit VIIb (Cox7b) proved to be induced (**Figure 1 E** and **Supplementary Table 2**). In contrast, proteins of the mitochondrial subcomplex IV were not dysregulated in the HC.

In addition, several proteins associated with ATP synthase (complex V) functionally linked with the electron transport chain and oxidative phosphorylation exhibited dysregulated expression levels in the PHC during the latency phase and during the chronic phase with recurrent spontaneous seizures. The analysis in PHC samples from the latency phase and chronic phase indicated reduced expression levels of ATP synthase, H+ transporting, mitochondrial F1 complex, O subunit (Atp5o) and ATP synthase, H+ transporting, mitochondrial F0 complex, subunit d (Atp5h) ten dpSE, and of Atp5h, ATP synthase, H+ transporting, mitochondrial F0 complex, subunit B1 (Atp5f1) and ATP synthase, H+ transporting, mitochondrial F1 complex, epsilon subunit pseudogene 2 (Atp5e) eight wpSE (**Figure 1 F, G** and **Supplementary Table 2**). In contrast, Atp5f1 exhibited elevated expression levels during the early post-insult and during the latency phase (**Figure 1 F, G** and **Supplementary Table 2**). In hippocampal tissue samples, the dysregulation of this subcategory of proteins was less pronounced. Only three proteins of complex V were up-regulated during the early post-insult phase: ATP synthase, H+ transporting, mitochondrial F1 complex, alpha subunit 1 (Atp5a1), ATP synthase, H+ transporting, mitochondrial F1 complex, beta polypeptide (Atp5b), and ATP synthase, H+ transporting, mitochondrial F1 complex, gamma polypeptide 1 (Atp5c1; **Figure 1 C** and **Supplementary Table 1**). However, Atp5a1 and Atp5b exhibited elevated expression levels in the PHC during the chronic epileptic phase (**Figure 1 G** and **Supplementary Table 2**).

For further information about differential expression of mitochondrial proteins see **Supplementary Tables 1** and **2**.

Regulation of proteins associated with calcium signaling

The calcium-binding regulatory protein calmodulin 1 (Calm1) was down-regulated in the PHC ten dpSE, while in the HC, expression rates of this protein were in the control range (**Figure 2 H-M)**.

A pronounced dysregulation of the protein phosphatase 3 (Ppp3) enzyme complex (the catalytic subunit of protein phosphatase 3 (formerly 2B) alpha and beta isoforms (Ppp3ca and Ppp3cb) and the regulatory subunit B of protein phosphatase 3 alpha isoform (Ppp3r1)) was evident during the time course of epileptogenesis. In hippocampal samples during the acute phase, Ppp3ca and Ppp3cb proved to be up-regulated, whereas during the latency phase all three proteins exhibited reduced expression levels in the HC and PHC. During the chronic phase expression rates of these proteins returned to control level, except for Ppp3cb which was up-regulated in the PHC (**Figure 2 H-M**).

Another protein associated with calcium signaling, inositol 1,4,5-triphosphate receptor type 1 (Itpr1), proved to be down-regulated during the early post-insult phase in hippocampal tissue samples and during the latency phase in both brain regions of interest (**Figure 2 H, I** and **L**). For further information about differential expression of proteins associated with calcium signaling see **Tables 1** and **2**.

Regulation of the microtubule-associated protein Tau

Differential proteomic analysis pointed to an epileptogenesis-associated downregulation of the microtubule-associated protein Tau in the PHC. In our data set we identified three different isoforms of the Tau (Mapt) protein: Mapt-001, Mapt-204 and Mapt-206 (**Figure 3).** Ten dpSE the expression of the isoform Mapt-204 was reduced by 1.2-fold in comparison with electrode-implanted control animals (**Figure 3 E** and **H)**. In apparent contrast, Tau exhibited no alterations in expression regulation in the HC (**Figure 3 A-C** and **G)**.

Considering the putative impact of Tau on excitability indicated by studies in genetic epilepsy models (Roberson et al., 2011, Holth et al., 2013, Gheyara et al., 2014, Zheng et al., 2014), we were interested to analyze the alterations in Tau expression patterns in more detail. Thus, we obtained region- and cell-specific information about Tau expression levels ten dpSE by immunohistochemistry.

In layer three of the posterior piriform cortex Tau expression proved to be significantly reduced ($p=0.038$), whereas in layers one and two Tau protein expression remained unaffected (layer one $p=0.330$ and layer 2 $p= 0.520$; data not shown). In the perirhinal cortex there was no decline in Tau expression, however in the entorhinal cortex the expression tended to be lower ($p= 0.057$; data not shown) in animals following SE when compared to electrode-implanted control animals. When all subregions of the PHC were analyzed together, Tau protein expression tended to be reduced. However, the difference failed to reach significance ($p=0.057$, **Figure 3 I**). Tau-positive neurons appeared as a ring-like structure with immunoreactivity in the cytoplasm and the neuronal processes. Tau-immunoreactivity of neurons was confirmed with NeuN double-staining. Quantification of Tau/NeuN double-labeled cells revealed that all neurons express Tau protein (data not shown). However, some Tau-immunopositive cells appeared in a glia-like morphology and were not labeled with the neuronal marker NeuN (**Figure J J,** black arrows).

Regulation of proteins associated with Aβ *processing, deposition, plaque formation, and* Aβ*-associated pathology*

In the PHC, we observed an early rise in Apolipoprotein E (ApoE) expression reaching a 3.4-fold upregulation 2 dpSE (**Figure 3 D** and **H**). During the latency phase and chronic epileptic phase with recurrent spontaneous seizures ApoE expression reached an even higher level in this brain region with a 6.2-fold and a 4.8-fold increased regulation when compared to electrode-implanted control animals (**Figure 3 E, F** and **H**). A delayed induction of ApoE was also evident in the HC with a 4.8-fold increase in the expression 10 dpSE (**Figure 3 B** and **G**). To validate proteomic ApoE expression data, we performed ApoE immunohistochemistry and analyzed the cellular expression by positive stained area and optical density in the HC 10 dpSE and at all three time points in parahippocampal cortex tissue.

In the HC we quantified the ApoE expression in the CA1 and CA3 region of the pyramidal layer of the cornu ammonis. Both brain hemispheres as well as the three analyzed regions along the rostro-caudal axis were analyzed together as there was no relevant difference. In the dentate gyrus and hilus of the HC we detected only diffuse positive signal, therefore a quantification was impossible. The positive labeled area as well as the optical density of immunopositive reaction was comparable in control and SE animals ten dpSE (CA1 area % $p = 0.5975$, OD $p = 0.8645$; CA3 area% $p = 0.4501$, OD $p = 0.6589$, **Figure 4, A-C**).

As there was no significant difference between the left and right hemisphere in the PHC we analyzed both sides together. In the rostral and caudal analyzed brain regions, we observed at all three analyzed time points comparable ApoE expression (area % and OD). ApoE expression in the medial analyzed region two dpSE showed a reduced ApoE positive area ($p = 0.0189$, **Figure 4, D and F**), whereas the optical density was increased in SE animals ($p = 0.0144$, **Figure 4, E and F**).

Both, App and alpha disintegrin metalloproteinase (Adam) 17 were differentially expressed during epileptogenesis. Whereas Adam17 was down-regulated in a pronounced manner in samples of the PHC during the latency phase, App proved to be induced in PHC tissue during the chronic phase of epilepsy (**Figure 3 E, F**).

Moreover, analysis of data sets from PHC tissue sampled during the latency phase revealed a 3.9-fold downregulation of α-synuclein (Snca, **Figure 3 E** and **H**).

Another protein of interest which is involved in Aβ clearing is the prolow-density lipoprotein receptor-related protein 1 (Lrp1) (Pflanzner et al., Whitfield, 2007). This protein exhibited increased expression rates in the HC ten dpSE and in the PHC eight wpSE (**Figure 3 B and F**).

For further information about differential expression of proteins associated with Aβ processing, deposition, plaque formation, and Aβ-associated pathology see **Tables 1** and **2**.

Discussion

The focused bioinformatics analysis confirmed our hypothesis that a relevant overlap exists in the dysregulation of proteins during epilepsy development following a brain insult and the dysregulation of proteins in AD and its progression.

Interestingly, the total number of proteins, which exhibits a dysregulation during epilepsy development as well as AD development, remained rather constant during the course of epileptogenesis from the early post-insult phase through the latency phase to the early phase following epilepsy manifestation. However, the individual proteins contributing to the overlap changed over time, with a persistent regulation of proteins at all investigated time points being rather an exception than the rule.

When comparing both brain areas, a more prominent regulation was evident in the samples comprising the posterior piriform cortex, entorhinal cortex and perirhinal cortex (referring to the PHC) as compared to the HC. This finding is of particular interest considering that parahippocampal subregions, and in particular the entorhinal cortex, are brain areas with an early manifestation of AD-associated neuropathological alterations (Krumm et al., 2016, Thaker et al., 2017). The more prominent epileptogenesis-associated dysregulation of proteins functionally linked with AD in the PHC, thus indicates that AD-like neuropathological alterations triggered by epileptogenic brain insults might also manifest earliest in parahippocampal subregions.

Mitochondrial dysfunction is a typical feature of AD pathophysiology (Picone et al., 2014, Cardoso et al., 2016). Respective findings have also triggered a particular interest in assessing mitochondria-targeted molecules as a basis for a pharmacological intervention in AD progression (Reddy and Reddy, 2017). The present study revealed a complex regulation of proteins associated with NADH dehydrogenase/ubiquinone regulation and function, cytochrome C oxidase subunit proteins, as well as proteins associated with ATP synthase, the electron transport chain and oxidative phosphorylation. Thus, proteins of the mitochondrial complex I, III, IV, V and the accessory subunit of complex I exhibited a dysregulation during the course of epileptogenesis and early phase following onset of recurrent seizures. The regulation was observed more prominent in the PHC than in the HC. The molecular alterations in mitochondrial proteins are likely contributors to epilepsy-specific synaptic pathology and the associated development of a persistent hyperexcitability via impaired calcium homeostasis (Chuang et al., 2004, Khurana et al., 2013, Walker, 2018). Whereas pronounced dysregulation of mitochondrial complex I, III and IV proteins was already

described during epileptogenesis and following epilepsy manifestation (Kudin et al., 2002, Chuang et al., 2004, Folbergrová et al., 2010, Ryan et al., 2012), less is known about the regulation of mitochondrial complex V proteins during epileptogenesis. Interestingly, in vitro data indicate that the mitochondrial complex V might play a crucial role in seizure-induced neuronal death (Kovac et al., 2012). Taking into account that mitochondrial abnormalities are considered relevant contributors to AD pathogenesis, the dysregulation of mitochondrial proteins following an epileptogenic brain insults might also constitute a factor contributing to AD-like pathologies in parahippocampal subregions, which develop following an epileptogenic insult.

One of the hypotheses for the development of AD is the "calcium hypothesis", which has been first raised by Khachaturian (1989) and has been recently revisited based on the current state-of-knowledge (Alzheimer's Association Calcium Hypothesis, 2017). The hypothesis proposes that calcium dyshomeostasis is the underlying cause for the disease (O'Day and Myre, 2004). Calmodulin is a Ca^{2+}-binding protein modulating the expression of other enzymes affecting calcium homeostasis such as the Ppp3 (also known as Calcineurin) (O'Day and Myre, 2004). Ppp3 has an impact on hippocampal long-term depression and might therefore be involved in the memory deficits characterizing AD (Xie, 2004, Zhang et al., 2015). Bioinformatic analysis of our data set revealed a complex dysregulation of various proteins playing a crucial role in calcium homeostasis. The dysregulation proved to be evident in both brain areas of interests, the HC and PHC. The list of proteins differentially expressed in at least one of the brain areas comprised Calm1, Ppp3ca, Ppp3cb, Ppp3r1, and Itpr1. Regulation of calmodulin and calcineurin has already been discussed in epileptology for several years (McNamara et al., 2006, Eckel et al., 2015, Liu et al., 2016). Very recently, the protein Itpr1 has been identified in epilepsy patients for the first time by whole-exome sequencing to be associated with sudden unexpected death in epilepsy (Friedman et al., 2018). Considering the "calcium hypothesis" of AD development (Khachaturian, 1989, Alzheimer's Association Calcium Hypothesis, 2017), the dysregulation of the proteins during epileptogenesis might not only contribute to changes in excitability as a hallmark of epilepsy development, but might also play an initial role in the manifestation of an AD-like pathology in structural epilepsies developing following a brain insult.

Alterations in Tau expression and deposition of Tau are one of the hallmarks in AD pathology (Liu and Gotz, 2013, Kalra and Khan, 2015, Li and Götz, 2017). Taking into consideration that alterations in Tau expression in some genetic models of epilepsy can affect network excitability (Holth et al., 2013, Gheyara et al., 2014), it is of particular interest to study the

dysregulation of Tau expression rates during the course of epileptogenesis. Our proteomic analysis revealed a down-regulation of Mapt-204 in the PHC ten dpSE. Quantification of Tau expression levels in parahippocampal subregions based on immunohistochemical stainings indicated that Tau is predominantly reduced in layer III of the posterior piriform cortex. In apparent contrast to our results, Miszczuk et al. (2016) reported a lack of changes in Tau gene expression rates during epileptogenesis in a mouse model of traumatic brain injury. Functional conclusions regarding a contribution of this molecular alteration are limited by the fact that we did not assess Tau hyperphosphorylation.

One of the major hallmarks in AD is the accumulation of senile plaques consisting of the Aβ peptide (Glenner and Wong, 1984, Roberson et al., 2011, Karran and De Strooper, 2016). Baldelli et al. (2010) reported that high levels of homocysteine, induced by the treatment with some antiepileptic drugs (Schwaninger et al., 1999), were found to promote Aβ deposition in the hippocampus and lowered the threshold to more severe seizures in the course of SE development in the pilocarpine model of TLE. Moreover, hyperhomocysteinemia is reported to be a risk factor for dementia (Selhub, 2008). This points towards the idea that Aβ deposition is not only a hallmark in AD but also plays an important role in the development of TLE. In line with this hypothesis, our bioinformatic analysis revealed a prominent regulation of several proteins being involved in Aβ processing and its regulation.

ApoE expression rates can affect Aβ metabolism and deposition, and amyloid pathology in a complex manner (Kanekiyo et al., 2014). Thereby, controversial findings have been reported with high as well as low levels of ApoE correlating with Aβ deposition (Mahoney-Sanchez et al., 2016). Among others, one explanation seems to be the different binding affinity of ApoE isoforms (Aleshkov et al., 1997, Tokuda et al., 2000). Whereas ApoE4 can increase the risk for Aβ deposition and aggregation (Schmechel et al., 1993, Polvikoski et al., 1995, Kok et al., 2009), ApoE2 and 3 isoforms can favor Aβ degradation and clearance (Deane et al., 2008, Jiang et al., 2008, Castellano et al., 2011). Moreover, it is known that inflammatory signaling can be triggered by ApoE (Tzioras et al., Dorey et al., 2014). A persistent induction of ApoE was evident in the PHC throughout the course of epileptogenesis and epilepsy manifestation. In addition, we observed an upregulation in the HC. Our data are in line with previous observations by Miszczuk et al. (2016) and Ni et al. (2013) describing an ApoE upregulation in two different epilepsy mouse models. Based on the complex role of ApoE, it is difficult to conclude about the consequences of ApoE overexpression during epileptogenesis. However, the trigger of inflammatory signaling by increased ApoE levels might definitely contribute to cellular and network alterations. In apparent contrast to our proteomic results, we were not

able to detect the up-regulation of ApoE expression on the cellular level. As we did not perfuse the rats that we used for the proteomic analysis but did for immunohistochemical analysis, this could have introduced confounders. Thus, conclusions regarding a contribution of this molecular alteration is still missing.

Altered processing of the App during AD pathogenesis can favor Aβ deposition (Nalivaeva and Turner, 2013). In the amyloidogenic pathway promoting Aβ deposition, App can undergo cleavage by β-secretase (= BACE)(Vassar et al., 2014). However, when exposed to α-secretase, i.e. Adam10 and 17, App can be processed in an alternate pathway, which can indirectly reduce deposition of neurotoxic Aβ (Kuhn et al., 2010). In the PHC App proved to be up-regulated in the chronic phase following epilepsy manifestation. These findings are in line with findings from a post-traumatic brain injury model of epileptogenesis in mice, in which a significant induction of App was observed (Miszczuk et al., 2016). Considering its role in the regulation of calcium homeostasis and the resulting neuroprotective function (Hefter and Draguhn, 2017), the induction of App might serve a beneficial role in the epileptic brain protecting neurons from the detrimental consequences of prolonged or repetitive seizures. On the other hand, higher concentrations of App imply enhanced levels of substrate for β- and γ-secretase generating Aβ. Thus, overexpression of App might be one factor contributing to AD-like neuropathological alterations in the epileptic brain.

Expression of the α-secretase Adam17 proved to be down-regulated in the PHC during the latency phase of epileptogenesis. As a direct implication more App is available for processing by β- and γ-secretase in the amyloidogenic pathway. Thus, low Adam17 expression during development of epilepsy might already trigger the development of an AD-like pathology. To our knowledge, regulation of Adam17 has not been intensely discussed previously in the context of epileptogenesis or epilepsy. Considering the important role of Adam17 in AD and the here reported regulation, it might be of interest to analyze the role of this protein during epileptogenesis in more detail in future studies.

The majority of patients with AD exhibit an accumulation of α-synuclein positive aggregates (Resende et al., 2013). An analysis of the interaction between α-synuclein and Aβ suggested that α-synuclein might protect against Aβ-triggered neuronal cell damage (Resende et al., 2013). Taking this finding into account, the low expression of α-synuclein evident in the PHC during the latency phase, might serve as an early contributor to AD-like pathological alterations during epileptogenesis. In apparent contrast to our findings, α-synuclein was elevated in serum and CSF of patients suffering from epilepsy as well as in the dentate gyrus in a mouse model of pilocarpine induced status epilepticus (Li et al., 2010, Rong et al., 2015).

Differences might be related to the disease phase under investigation as well as the model and species used in the experimental study.

As mentioned above, Lrp1 also contributes to Aβ clearing (Pflanzner et al., Whitfield, 2007). Knockout of astrocytic Lrp1 is associated with reduced cellular uptake and intracellular degradation of Aβ as well as accelerated Aβ accumulation and plaque formation in an AD mouse model (Liu et al., 2017). Increased expression levels of Lrp1 observed ten dpSE in the HC and eight wpSE in the PHC might thus counteract Aβ deposition. To our knowledge, Lrp1 regulation has not been discussed in earlier studies of epileptogenesis or epilepsy. Considering the functional role of Lrp1, it might be of interest to further study the functional consequences of its regulation during epileptogenesis.

A limitation of our study might be the use of female rats. However, we know from several years of experience that the mortality of male rats is quite high in the electrical post-status-epilepticus model (Brandt et al., 2003). Therefore, the animal numbers have to be dramatically increased to gain reliable results. This faces ethical concerns. Moreover, the NIH criticized the overrepresentation of male animals in preclinical studies and requested a gender balance and the inclusion of female animals in future studies (Clayton and Collins, 2014). Furthermore, female rats have been chosen for this study as we expect a higher variance in female rats related to the estrous cycle, and our long-term aim is to identify robust protein expression alterations. For the above-mentioned reasons we decided to use female rats in this first study. However, it will be of future interest to perform a comparative study in male rats.

We have to acknowledge that further validation by immonhistochemistry of some AD-related protein findings failed to be successful. This might be due to the reason that we did not perfuse the rats used for the proteomics analysis. This could introduce confounders regarding the validation.

In conclusion, the focused bioinformatics analysis of proteomic data sets obtained from two brain areas during the course of epileptogenesis revealed a relevant regulation of proteins known to be associated with AD pathogenesis. Therewith, the analysis provided an overview of the overlap in molecular alterations characterizing epilepsy development and manifestation on the one hand and AD development and progression on the other hand. Any conclusion from the proteomic data needs to take into account that the regulation of individual proteins will require further confirmation. Moreover, it will be of particular interest to study the regulation of different isoforms and phosphorylation states of selected proteins in future studies.

However, at the current stage our findings already provide a very valuable and comprehensive basis for the generation of novel hypothesis regarding shared molecular events in both disease states.

Acknowledgements

The authors thank Fabian Gruhn, Sandra Helm, and Claudia Siegl for their excellent technical assistance.

Funding: Research in H. Potschka's group has been and is supported by grants of the Deutsche Forschungsgemeinschaft (DFG PO 681/5-2 and PO 681/8-1).

Author Contributions:

EL von Rüden: Data analysis and statistics, immunohistochemistry, critical discussion of the results and writing of the manuscript

C Zellinger: Data analysis and critical reading of the manuscript

J Gedon: ApoE immunohistochemistry and quantification, critical reading of the manuscript

A Walker: Animal experiments, data analysis of raw data and critical reading of the manuscript

V Bierling: Animal experiments, data analysis of raw data and critical reading of the manuscript

CA Deeg: Study design, data analysis of raw data and critical reading of the manuscript

SM Hauck: Study design, data analysis of raw data and critical reading of the manuscript

H Potschka: Study concept and design, critical discussion of the results and writing of the manuscript

Declaration of interest: none

References

Aleshkov S, Abraham CR, Zannis VI (1997) Interaction of nascent ApoE2, ApoE3, and ApoE4 isoforms expressed in mammalian cells with amyloid peptide beta (1-40). Relevance to Alzheimer's disease. Biochemistry 36:10571-10580.

Alzheimer's Association Calcium Hypothesis W (2017) Calcium Hypothesis of Alzheimer's disease and brain aging: A framework for integrating new evidence into a comprehensive theory of pathogenesis. Alzheimers Dement 13:178-182.e117.

Baldelli E, Leo G, Andreoli N, Fuxe K, Biagini G, Agnati LF (2010) Homocysteine Potentiates Seizures and Cell Loss Induced by Pilocarpine Treatment. NeuroMolecular Medicine 12:248-259.

Brandt C, Glien M, Potschka H, Volk H, Loscher W (2003) Epileptogenesis and neuropathology after different types of status epilepticus induced by prolonged electrical stimulation of the basolateral amygdala in rats. Epilepsy Res 55:83-103.

Cardoso S, Carvalho C, Correia SC, Seiça RM, Moreira PI (2016) Alzheimeŕs disease: From mitochondrial perturbations to mitochondrial medicine. Brain Pathol.

Castellano JM, Kim J, Stewart FR, Jiang H, DeMattos RB, Patterson BW, Fagan AM, Morris JC, et al. (2011) Human apoE isoforms differentially regulate brain amyloid-β peptide clearance. Sci transl med 3:89ra57-89ra57.

Chen C, Holth JK, Bunton-Stasyshyn R, Anumonwo CK, Meisler MH, Noebels JL, Isom LL (2018) Mapt deletion fails to rescue premature lethality in two models of sodium channel epilepsy. Ann Clin Transl Neurol 5:982-987.

Chuang YC, Chang AY, Lin JW, Hsu SP, Chan SH (2004) Mitochondrial dysfunction and ultrastructural damage in the hippocampus during kainic acid-induced status epilepticus in the rat. Epilepsia 45:1202-1209.

Cirrito JR, Kang JE, Lee J, Stewart FR, Verges DK, Silverio LM, Bu G, Mennerick S, et al. (2008) Endocytosis is required for synaptic activity-dependent release of amyloid-beta in vivo. Neuron 58:42-51.

Cirrito JR, Yamada KA, Finn MB, Sloviter RS, Bales KR, May PC, Schoepp DD, Paul SM, et al. (2005) Synaptic activity regulates interstitial fluid amyloid-beta levels in vivo. Neuron 48:913-922.

Clayton JA, Collins FS (2014) Policy: NIH to balance sex in cell and animal studies. Nature 509:282-283.

de Guzman P, Inaba Y, Baldelli E, de Curtis M, Biagini G, Avoli M (2008) Network hyperexcitability within the deep layers of the pilocarpine-treated rat entorhinal cortex. The Journal of physiology 586:1867-1883.

de Lanerolle NC, Kim JH, Robbins RJ, Spencer DD (1989) Hippocampal interneuron loss and plasticity in human temporal lobe epilepsy. Brain Res 495:387-395.

Deane R, Sagare A, Hamm K, Parisi M, Lane S, Finn MB, Holtzman DM, Zlokovic BV (2008) apoE isoform–specific disruption of amyloid β peptide clearance from mouse brain. J Clin Invest 118:4002-4013.

Dorey E, Chang N, Liu QY, Yang Z, Zhang W (2014) Apolipoprotein E, amyloid-beta, and neuroinflammation in Alzheimer's disease. Neurosci Bull 30:317-330.

Du F, Eid T, Lothman EW, Kohler C, Schwarcz R (1995) Preferential neuronal loss in layer III of the medial entorhinal cortex in rat models of temporal lobe epilepsy. The Journal of Neuroscience 15:6301.

Eckel R, Szulc B, Walker MC, Kittler JT (2015) Activation of calcineurin underlies altered trafficking of α2 subunit containing GABA(A) receptors during prolonged epileptiform activity. Neuropharmacology 88:82-90.

Folbergrová J, Ješina P, Haugvicová R, Lisý V, Houštěk J (2010) Sustained deficiency of mitochondrial complex I activity during long periods of survival after seizures induced in immature rats by homocysteic acid. Neurochem Int 56:394-403.

Friedman D, Kannan K, Faustin A, Shroff S, Thomas C, Heguy A, Serrano J, Snuderl M, et al. (2018) Cardiac arrhythmia and neuroexcitability gene variants in resected brain tissue from patients with sudden unexpected death in epilepsy (SUDEP). NPJ Genom Med 3:9.

Gan L, Qiao S, Lan X, Chi L, Luo C, Lien L, Liu QY, Liu R (2008) Neurogenic Responses to Amyloid-Beta Plaques in the Brain of Alzheimer's Disease-Like Transgenic (pPDGF-APP(Sw,Ind)) Mice. Neurobiol Dis 29:71-80.

Gheyara AL, Ponnusamy R, Djukic B, Craft RJ, Ho K, Guo W, Finucane MM, Sanchez PE, et al. (2014) Tau Reduction Prevents Disease in a Mouse Model of Dravet Syndrome. Ann Neurol 76:443-456.

Glenner GG, Wong CW (1984) Alzheimer's disease: Initial report of the purification and characterization of a novel cerebrovascular amyloid protein. Biochem Bioph Res Co 120:885-890.

Hefter D, Draguhn A (2017) APP as a Protective Factor in Acute Neuronal Insults. Front Mol Neurosci 10:22.

Holth JK, Bomben VC, Reed JG, Inoue T, Younkin L, Younkin SG, Pautler RG, Botas J, et al. (2013) Tau loss attenuates neuronal network hyperexcitability in mouse and Drosophila genetic models of epilepsy. J Neurosci 33:1651-1659.

Jiang Q, Lee CY, Mandrekar S, Wilkinson B, Cramer P, Zelcer N, Mann K, Lamb B, et al. (2008) ApoE promotes the proteolytic degradation of Abeta. Neuron 58:681-693.

Jin K, Peel AL, Mao XO, Xie L, Cottrell BA, Henshall DC, Greenberg DA (2004) Increased hippocampal neurogenesis in Alzheimer's disease. P Natl Acad Sci USA 101:343-347.

Kalra J, Khan A (2015) Reducing Abeta load and tau phosphorylation: Emerging perspective for treating Alzheimer's disease. Eur J Pharmacol 764:571-581.

Kandratavicius L, Monteiro MR, Hallak JE, Carlotti CG, Assirati JA, Leite JP (2013) Microtubule-Associated Proteins in Mesial Temporal Lobe Epilepsy with and without Psychiatric Comorbidities and Their Relation with Granular Cell Layer Dispersion. BioMed Research International 2013:960126.

Kanehisa M, Furumichi M, Tanabe M, Sato Y, Morishima K (2017) KEGG: new perspectives on genomes, pathways, diseases and drugs. Nucleic Acids Research 45:D353-D361.

Kanehisa M, Goto S (2000) KEGG: Kyoto Encyclopedia of Genes and Genomes. Nucleic Acids Res 28:27-30.

Kanehisa M, Sato Y, Kawashima M, Furumichi M, Tanabe M (2016) KEGG as a reference resource for gene and protein annotation. Nucleic Acids Res 44:D457-D462.

Kanekiyo T, Xu H, Bu G (2014) ApoE and Aβ in Alzheimer's disease: accidental encounters or partners? Neuron 81:740-754.

Karran E, De Strooper B (2016) The amyloid cascade hypothesis: are we poised for success or failure? J Neurochem 139 Suppl 2:237-252.

Keck M, Androsova G, Gualtieri F, Walker A, von Ruden EL, Russmann V, Deeg CA, Hauck SM, et al. (2017) A systems level analysis of epileptogenesis-associated proteome alterations. Neurobiol Dis.

Keck M, van Dijk RM, Deeg CA, Kistler K, Walker A, von Rüden E-L, Russmann V, Hauck SM, et al. (2018) Proteomic profiling of epileptogenesis in a rat model: Focus on cell stress, extracellular matrix and angiogenesis. Neurobiology of Disease 112:119-135.

Khachaturian ZS (1989) Calcium, membranes, aging, and Alzheimer's disease. Introduction and overview. Ann N Y Acad Sci 568:1-4.

Khurana DS, Valencia I, Goldenthal MJ, Legido A (2013) Mitochondrial Dysfunction in Epilepsy. Semin Pediatr Neurol 20:176-187.

Kok E, Haikonen S, Luoto T, Huhtala H, Goebeler S, Haapasalo H, Karhunen PJ (2009) Apolipoprotein E-dependent accumulation of Alzheimer disease-related lesions begins in middle age. Ann Neurol 65:650-657.

Kovac S, Domijan A-M, Walker MC, Abramov AY (2012) Prolonged seizure activity impairs mitochondrial bioenergetics and induces cell death. J cell sci 125:1796-1806.

Krumm S, Kivisaari SL, Probst A, Monsch AU, Reinhardt J, Ulmer S, Stippich C, Kressig RW, et al. (2016) Cortical thinning of parahippocampal subregions in very early Alzheimer's disease. Neurobiol Aging 38:188-196.

Kudin AP, Kudina TA, Seyfried J, Vielhaber S, Beck H, Elger CE, Kunz WS (2002) Seizure-dependent modulation of mitochondrial oxidative phosphorylation in rat hippocampus. Eur J Neurosci 15:1105-1114.

Kuhn P-H, Wang H, Dislich B, Colombo A, Zeitschel U, Ellwart JW, Kremmer E, Roßner S, et al. (2010) ADAM10 is the physiologically relevant, constitutive α-secretase of the amyloid precursor protein in primary neurons. The EMBO Journal 29:3020-3032.

Larner AJ (2010) Epileptic Seizures in AD Patients. Neuro Mol Med 12:71-77.

Lesné S, Ali C, Gabriel C, Croci N, MacKenzie ET, Glabe CG, Plotkine M, Marchand-Verrecchia C, et al. (2005) NMDA Receptor Activation Inhibits α-Secretase and Promotes Neuronal Amyloid-β Production. J Neurosci 25:9367-9377.

Li A, Choi Y-S, Dziema H, Cao R, Cho H-Y, Jung YJ, Obrietan K (2010) Proteomic profiling of the epileptic dentate gyrus. Brain pathol 20:1077-1089.

Li C, Götz J (2017) Tau-based therapies in neurodegeneration: opportunities and challenges. Nature Reviews Drug Discovery 16:863.

Liu C, Gotz J (2013) How it all started: tau and protein phosphatase 2A. J Alzheimers Dis 37:483-494.

Liu CC, Hu J, Zhao N, Wang J, Na W, Cirrito JR, Kanekiyo T, Holtzman DM, et al. (2017) Astrocytic LRP1 Mediates Brain Abeta Clearance and Impacts Amyloid Deposition. J Neurosci.

Liu J, Li X, Chen L, Xue P, Yang Q, Wang A (2016) Increased calcineurin expression after pilocarpine-induced status epilepticus is associated with brain focal edema and astrogliosis. Int J Neurosci 126:560-567.

Mahoney-Sanchez L, Belaidi AA, Bush AI, Ayton S (2016) The Complex Role of Apolipoprotein E in Alzheimer's Disease: an Overview and Update. J Mol Neurosci 60:325-335.

McNamara JO, Huang YZ, Leonard AS (2006) Molecular signaling mechanisms underlying epileptogenesis. Sci STKE 2006:re12.

Merl J, Ueffing M, Hauck SM, von Toerne C (2012) Direct comparison of MS-based label-free and SILAC quantitative proteome profiling strategies in primary retinal Müller cells. Proteomics 12:1902-1911.

Minkeviciene R, Rheims S, Dobszay MB, Zilberter M, Hartikainen J, Fülöp L, Penke B, Zilberter Y, et al. (2009) Amyloid β-Induced Neuronal Hyperexcitability Triggers Progressive Epilepsy. J Neurosci 29:3453-3462.

Miszczuk D, Dębski KJ, Tanila H, Lukasiuk K, Pitkänen A (2016) Traumatic Brain Injury Increases the Expression of Nos1, Aβ Clearance, and Epileptogenesis in APP/PS1 Mouse Model of Alzheimer's Disease. Mol Neurobiol 53:7010-7027.

Nalivaeva NN, Turner AJ (2013) The amyloid precursor protein: A biochemical enigma in brain development, function and disease. FEBS Lett 587:2046-2054.

Ni H, Ren S-y, Zhang L-l, Sun Q, Tian T, Feng X (2013) Expression profiles of hippocampal regenerative sprouting-related genes and their regulation by E-64d in a developmental rat model of penicillin-induced recurrent epilepticus. Toxicol Lett 217:162-169.

Nicastro N, Assal F, Seeck M (2016) From here to epilepsy: the risk of seizure in patients with Alzheimer's disease. Epileptic Disord 18:1-12.

Noble W, Planel E, Zehr C, Olm V, Meyerson J, Suleman F, Gaynor K, Wang L, et al. (2005) Inhibition of glycogen synthase kinase-3 by lithium correlates with reduced tauopathy and degeneration in vivo. P Natl Acad Sci USA 102:6990-6995.

Noebels JL (2011) A Perfect Storm: Converging Paths of Epilepsy and Alzheimer's Dementia Intersect in the Hippocampal Formation. Epilepsia 52:39-46.

O'Day DH, Myre MA (2004) Calmodulin-binding domains in Alzheimer's disease proteins: extending the calcium hypothesis. Biochem Bioph Res Co 320:1051-1054.

Palop JJ, Mucke L (2009) Epilepsy and Cognitive Impairments in Alzheimer Disease. Arch Neurol-Chicago 66:435.

Parent JM, Murphy GG (2008) Mechanisms and functional significance of aberrant seizure-induced hippocampal neurogenesis. Epilepsia 49 Suppl 5:19-25.

Paxinos G, Watson C (1998) The Rat Brain in Stereotactic Coordinates. Academic Press, Sydney.

Pflanzner T, Janko MC, André-Dohmen B, Reuss S, Weggen S, Roebroek AJM, Kuhlmann CRW, Pietrzik CU LRP1 mediates bidirectional transcytosis of amyloid-β across the blood-brain barrier. Neurobiol Aging 32:2323.e2321-2323.e2311.

Picone P, Nuzzo D, Caruana L, Scafidi V, Di Carlo M (2014) Mitochondrial Dysfunction: Different Routes to Alzheimer’s Disease Therapy. Oxid Med Cell Longev 2014:11.

Polvikoski T, Sulkava R, Haltia M, Kainulainen K, Vuorio A, Verkkoniemi A, Niinistö L, Halonen P, et al. (1995) Apolipoprotein E, Dementia, and Cortical Deposition of β-Amyloid Protein. New Engl J Med 333:1242-1248.

Racine RJ (1972) Modification of seizure activity by electrical stimulation. II. Motor seizure. Electroencephalography and clinical neurophysiology 32:281-294.

Rauramaa T, Saxlin A, Lohvansuu K, Alafuzoff I, Pitkänen A, Soininen H (2018) Epilepsy in neuropathologically verified Alzheimer's disease. Seizure 58:9-12.

Reddy AP, Reddy PH (2017) Chapter Six - Mitochondria-Targeted Molecules as Potential Drugs to Treat Patients With Alzheimer's Disease. In: Progress in Molecular Biology and Translational Science, vol. Volume 146 (Reddy, P. H., ed), pp 173-201: Academic Press.

Resende R, Marques SCF, Ferreiro E, Simões I, Oliveira CR, Pereira CMF (2013) Effect of α-Synuclein on Amyloid β-Induced Toxicity: Relevance to Lewy Body Variant of Alzheimer Disease. Neurochem Res 38:797-806.

Reyes-Marin KE, Nuñez A (2017) Seizure susceptibility in the APP/PS1 mouse model of Alzheimer's disease and relationship with amyloid β plaques. Brain Research 1677:93-100.

Roberson ED, Halabisky B, Yoo JW, Yao J, Chin J, Yan F, Wu T, Hamto P, et al. (2011) Amyloid-β/Fyn–Induced Synaptic, Network, and Cognitive Impairments Depend on Tau Levels in Multiple Mouse Models of Alzheimer's Disease. The Journal of Neuroscience 31:700-711.

Rong H, Jin L, Wei W, Wang X, Xi Z (2015) Alpha-synuclein is a potential biomarker in the serum and CSF of patients with intractable epilepsy. Seizure 27:6-9.

Russmann V, Goc J, Boes K, Ongerth T, Salvamoser JD, Siegl C, Potschka H (2016) Minocycline fails to exert antiepileptogenic effects in a rat status epilepticus model. Eur J Pharmacol 771:29-39.

Ryan K, Backos DS, Reigan P, Patel M (2012) Post-Translational Oxidative Modification and Inactivation of Mitochondrial Complex I in Epileptogenesis. J Neurosci 32:11250-11258.

Scharfman HE, Chao MV (2013) The entorhinal cortex and neurotrophin signaling in Alzheimer's disease and other disorders. Cogn Neurosci 4:123-135.

Schmechel DE, Saunders AM, Strittmatter WJ, Crain BJ, Hulette CM, Joo SH, Pericak-Vance MA, Goldgaber D, et al. (1993) Increased amyloid beta-peptide deposition in cerebral cortex as a consequence of apolipoprotein E genotype in late-onset Alzheimer disease. P Natl Acad Sci USA 90:9649-9653.

Schoch Kathleen M, DeVos Sarah L, Miller Rebecca L, Chun Seung J, Norrbom M, Wozniak David F, Dawson Hana N, Bennett CF, et al. (2016) Increased 4R-Tau Induces Pathological Changes in a Human-Tau Mouse Model. Neuron 90:941-947.

Schwaninger M, Ringleb P, Winter R, Kohl B, Fiehn W, Rieser PA, Walter-Sack I (1999) Elevated plasma concentrations of homocysteine in antiepileptic drug treatment. Epilepsia 40:345-350.

Selhub J (2008) Public health significance of elevated homocysteine. Food Nutr Bull 29:S116-125.

Sutula TP, Dudek FE (2007) Unmasking recurrent excitation generated by mossy fiber sprouting in the epileptic dentate gyrus: an emergent property of a complex system. In: Prog Brain Res, vol. Volume 163 (Helen, E. S., ed), pp 541-563: Elsevier.

Tai XY, Koepp M, Duncan JS, Fox N, Thompson P, Baxendale S, Liu JY, Reeves C, et al. (2016) Hyperphosphorylated tau in patients with refractory epilepsy correlates with cognitive decline: a study of temporal lobe resections. Brain 139:2441-2455.

Thaker AA, Weinberg BD, Dillon WP, Hess CP, Cabral HJ, Fleischman DA, Leurgans SE, Bennett DA, et al. (2017) Entorhinal Cortex: Antemortem Cortical Thickness and Postmortem Neurofibrillary Tangles and Amyloid Pathology. AM J Neuroradiol.

Tokuda T, Calero M, Matsubara E, Vidal R, Kumar A, Permanne B, Zlokovic B, Smith JD, et al. (2000) Lipidation of apolipoprotein E influences its isoform-specific interaction with Alzheimer's amyloid beta peptides. Biochemical J 348:359-365.

Tzioras M, Davies C, Newman A, Jackson R, Spires-Jones T APOE at the interface of inflammation, neurodegeneration and pathological protein spread in Alzheimer's disease. Neuropathology and Applied Neurobiology 0.

Uhl PB, Szober CM, Amann B, Alge-Priglinger C, Ueffing M, Hauck SM, Deeg CA (2014) In situ cell surface proteomics reveals differentially expressed membrane proteins in retinal pigment epithelial cells during autoimmune uveitis. J Proteomics 109:50-62.

Vassar R, Kuhn P-H, Haass C, Kennedy ME, Rajendran L, Wong PC, Lichtenthaler SF (2014) Function, therapeutic potential and cell biology of BACE proteases: current status and future prospects. J Neurochem 130:4-28.

Volk HA, Potschka H, Löscher W (2004) Increased expression of the multidrug transporter P-glycoprotein in limbic brain regions after amygdala-kindled seizures in rats. Epilepsy Research 58:67-79.

Walker A, Russmann V, Deeg CA, von Toerne C, Kleinwort KJ, Szober C, Rettenbeck ML, von Ruden EL, et al. (2016) Proteomic profiling of epileptogenesis in a rat model: Focus on inflammation. Brain Behav Immun 53:138-158.

Walker MC (2018) Pathophysiology of status epilepticus. Neuroscience Letters 667:84-91.

Whitfield JF (2007) The road to load late-onset Alzheimer's disease and a possible way to block it. Expert Opin Ther Tar 11:1257-1260.

Wisniewski JR, Zougman A, Nagaraj N, Mann M (2009) Universal sample preparation method for proteome analysis. Nat Meth 6:359-362.

Xie C-W (2004) Calcium-regulated signaling pathways. Neuromol Med 6:53-64.

Xu W, Fitzgerald S, Nixon RA, Levy E, Wilson DA (2015) Early hyperactivity in lateral entorhinal cortex is associated with elevated levels of AbetaPP metabolites in the Tg2576 mouse model of Alzheimer's disease. Exp Neurol 264:82-91.

Zhang H, Liu J, Sun S, Pchitskaya E, Popugaeva E, Bezprozvanny I (2015) Calcium signaling, excitability and synaptic plasticity defects in mouse model of Alzheimer’s disease. J Alzheimers dis 45:561-580.

Zheng P, Shultz SR, Hovens CM, Velakoulis D, Jones NC, O’Brien TJ (2014) Hyperphosphorylated Tau is Implicated in Acquired Epilepsy and Neuropsychiatric Comorbidities. Mol Neurobiol 49:1532-1539.

Zumkehr J, Rodriguez-Ortiz CJ, Cheng D, Kieu Z, Wai T, Hawkins C, Kilian J, Lim SL, et al. Ceftriaxone ameliorates tau pathology and cognitive decline via restoration of glial glutamate transporter in a mouse model of Alzheimer's disease. Neurobiol Aging 36:2260-2271.

Tables

Table 1

#	Identified protein	Accession codea	Peptides used for quantificationb	Confidence Scorec	Anova (p)d	Fold change
		2 days post SE				
1	Succinate dehydrogenase complex, subunit C	ENSRNOP00000004228	3	123	0.032	2.0
2	NADH dehydrogenase (ubiquinone) 1 beta subcomplex 8	ENSRNOP00000019039	7	364	0.011	1.4
3	NADH dehydrogenase (ubiquinone) 1 beta subcomplex, 5	ENSRNOP00000016051	4	154	6.08E-04	1.4
4	Ubiquinol-cytochrome c reductase, Rieske iron-sulfur polypeptide 1	ENSRNOP00000024609	9	492	2.58E-04	1.4
5	Guanine nucleotide binding protein (G protein), q polypeptide	ENSRNOP00000019174	6	545	0.003	1.3
6	ATP synthase, H+ transporting, mitochondrial F1 complex, gamma polypeptide 1	ENSRNOP00000061946	11	544	6.90E-05	1.3
7	NADH dehydrogenase (ubiquinone) 1 beta subcomplex, 7	ENSRNOP00000034511	5	210	0.004	1.3
8	ATP synthase, H+ transporting, mitochondrial F1 complex, beta polypeptide	ENSRNOP00000003965	47	3892	0.005	1.3
9	Succinate dehydrogenase complex, subunit B, iron sulfur	ENSRNOP00000010593	9	424	0.010	1.2
10	Cytochrome c oxidase subunit IV isoform 1	ENSRNOP00000024033	8	387	0.045	1.2

Regulated proteins of the AD pathway in the HC ranked by fold change (relation of relative protein abundances between control and animals post SE). There are no proteins regulated at 8 weeks post SE.

[a] Accession number of identified proteins as given in Ensembl protein database (http://www.ensembl.org)

Thresholds were set at: [b] Peptides used for quantification > 2, [c] Confidence score > 30 and [d] p-value < 0.05

S: Surfaceome; N: nucleus; C: cytoplasm.

Table 1
Continuation

#	Identified protein	Accession codea	Peptides used for quantificationb	Confidence Scorec	Anova (p)d	Fold change
		2 days post SE				
11	ATP synthase, H+ transporting, mitochondrial F1 complex, alpha subunit 1, cardiac muscle	ENSRNOP00000022892	36	2856	0.002	1.2
12	Serine/threonine-protein phosphatase 2B catalytic subunit alpha isoform	ENSRNOP00000013305	16	1436	0.010	1.2
13	Cytochrome b-c1 complex subunit 2, mitochondrial	ENSRNOP00000021514	27	1505	0.003	1.1
14	Mitogen-activated protein kinase 3	ENSRNOP00000026627	6	763	0.024	1.1
15	Serine/threonine-protein phosphatase 2B catalytic subunit beta isoform	ENSRNOP00000010476	6	842	0.018	1.1
16	Succinate dehydrogenase [ubiquinone] flavoprotein subunit, mitochondrial	ENSRNOP00000018336	27	1646	0.037	1.1
17	Cytochrome c-1 (Predicted), isoform CRA_cUncharacterized protein	ENSRNOP00000017067	11	699	0.004	1.1
18	NADH dehydrogenase (ubiquinone) 1 alpha subcomplex, 6 (B14)	ENSRNOP00000011484	2	224	0.024	-1.2
		10 days post SE				
1	Apolipoprotein E	ENSRNOP00000050968	15	840	0.038	4.8
2	Inositol 1,4,5-trisphosphate receptor type 1	ENSRNOP00000009288	7	260	0.037	-1.6
3	Glyceraldehyde-3-phosphate dehydrogenase	ENSRNOP00000040878	8	1912	1.76E-03	-1.3
4	Serine/threonine-protein phosphatase 2B catalytic subunit alpha isoform	ENSRNOP00000013305	16	1436	0.038	-1.2
5	Serine/threonine-protein phosphatase 2B catalytic subunit beta isoform	ENSRNOP00000010476	6	842	0.044	-1.2

Regulated proteins of the AD pathway in the HC ranked by fold change (relation of relative protein abundances between control and animals post SE). There are no proteins regulated at 8 weeks post SE.

[a] Accession number of identified proteins as given in Ensembl protein database (http://www.ensembl.org)

Thresholds were set at: [b] Peptides used for quantification > 2, [c] Confidence score > 30 and [d] p-value < 0.05

S: Surfaceome; N: nucleus; C: cytoplasm.

Table 2

#	Gene Symbol	Accession codea	Peptides used for quantificationb	Confidence Scorec	Anova (p)d	Fold change
		2 days post SE				
1	Apolipoprotein E	ENSRNOP00000050968	17	976	8.61E-05	3.40
2	Cytochrome c oxidase, subunit VIa, polypeptide 1	ENSRNOP00000001545	2	130	0.026	1.70
3	Succinate dehydrogenase complex, subunit D, integral membrane protein	ENSRNOP00000034407	2	90	0.023	1.70
4	Cytochrome c oxidase subunit VIIb	ENSRNOP00000054370	2	67	0.04	1.60
5	NADH dehydrogenase (ubiquinone) 1 alpha subcomplex, 6	ENSRNOP00000011484	2	224	0.005	1.60
6	ATP synthase, H+ transporting, mitochondrial Fo complex, subunit B1	ENSRNOP00000021920	13	614	4.94E-04	1.30
7	NEDD8-activating enzyme E1 regulatory subunit	ENSRNOP00000045593	2	85	2.69E-04	1.30
8	Ubiquinol-cytochrome c reductase core protein I	ENSRNOP00000044696	24	1643	0.002	1.30
9	Cytochrome c-1	ENSRNOP00000017067	13	778	0.006	1.20
10	NADH dehydrogenase (ubiquinone) 1 beta subcomplex 4	ENSRNOP00000003674	5	182	0.003	1.20
11	Cytochrome c oxidase, subunit VIc	ENSRNOP00000014407	5	191	0.028	1.10
12	NADH dehydrogenase (ubiquinone) Fe-S protein 7	ENSRNOP00000037256	7	455	0.004	1.10
13	Ubiquinol cytochrome c reductase core protein 2	ENSRNOP00000021514	28	1553	0.008	1.10
14	Glycogen synthase kinase 3 beta	ENSRNOP00000003867	4	224	0.024	-1.20
15	Guanine nucleotide binding protein (G protein), q polypeptide	ENSRNOP00000019174	7	635	7.16E-04	-1.30
16	Inositol 1,4,5-trisphosphate receptor type 1	ENSRNOP00000009288	5	230	0.005	-1.60

Regulated proteins of the AD pathway in the PHC ranked by fold change (relation of relative protein abundances between control and animals post SE). There are no proteins regulated at 8 weeks post SE.

[a] Accession number of identified proteins as given in Ensembl protein database (http://www.ensembl.org)

Thresholds were set at: [b] Peptides used for quantification > 2, [c] Confidence score > 30 and [d] p-value < 0.05

S: Surfaceome; N: nucleus; C: cytoplasm.

Table 2
Continuation

#	Gene Symbol	Accession codea	Peptides used for quantificationb	Confidence Scorec	Anova (p)d	Fold change
		10 days post SE				
1	Apolipoprotein E	ENSRNOP00000050968	17	976	1.80E-05	6.20
2	NADH dehydrogenase (ubiquinone) 1, subcomplex unknown, 2	ENSRNOP00000016509	2	176	0.016	1.70
3	NEDD8 activating enzyme E1 subunit 1	ENSRNOP00000045593	2	85	0.021	1.40
4	Hydroxysteroid (17-beta) dehydrogenase 10	ENSRNOP00000043608	9	658	0.005	1.30
5	NADH dehydrogenase (ubiquinone) 1 alpha subcomplex 6	ENSRNOP00000011484	2	224	0.025	1.30
6	NADH dehydrogenase (ubiquinone) Fe-S protein 3	ENSRNOP00000012425	9	519	0.005	1.30
7	ubiquinol-cytochrome c reductase core protein II	ENSRNOP00000021514	28	1553	0.001	1.30
8	ubiquinol-cytochrome c reductase, complex III subunit VII	ENSRNOP00000009547	3	140	0.047	1.30
9	ATP synthase, H+ transporting, mitochondrial Fo complex, subunit B1	ENSRNOP00000021920	13	614	0.008	1.20
10	Cytochrome c-1	ENSRNOP00000017067	13	778	0.004	1.20
11	ubiquinol-cytochrome c reductase core protein I	ENSRNOP00000044696	24	1643	0.008	1.20
12	Cytochrome c oxidase subunit 7A-related protein, mitochondrial	ENSRNOP00000005970	4	198	0.006	1.10
13	NADH dehydrogenase (ubiquinone) flavoprotein 1	ENSRNOP00000024517	19	1177	0.045	-1.20
14	protein phosphatase 3 (formerly 2B), catalytic subunit, alpha isoform	ENSRNOP00000013305	13	1435	0.004	-1.20
15	protein phosphatase 3 (formerly 2B), catalytic subunit, beta isoform	ENSRNOP00000010476	9	928	0.003	-1.20
16	succinate dehydrogenase complex, subunit B	ENSRNOP00000010593	8	349	0.031	-1.20
17	Glyceraldehyde-3-phosphate dehydrogenase	ENSRNOP00000040878	7	2186	0.004	-1.30
18	phospholipase C, beta 1	ENSRNOP00000042533	8	2133	0.013	-1.30

Regulated proteins of the AD pathway in the PHC ranked by fold change (relation of relative protein abundances between control and animals post SE). There are no proteins regulated at 8 weeks post SE.

[a] Accession number of identified proteins as given in Ensembl protein database (http://www.ensembl.org)

Thresholds were set at: [b] Peptides used for quantification > 2, [c] Confidence score > 30 and [d] p-value < 0.05

S: Surfaceome; N: nucleus; C: cytoplasm.

Table 2
Continuation

#	Gene Symbol	Accession codea	Peptides used for quantificationb	Confidence Scorec	Anova (p)d	Fold change
		10 days post SE				
19	Guanine nucleotide binding protein (G protein), q polypeptide	ENSRNOP00000019174	7	635	0.01	-1.40
20	ATP synthase, H+ transporting, mitochondrial F1 complex, O subunit	ENSRNOP00000002732	11	773	0.009	-1.50
21	NADH Dehydrogenase (ubiquinone) Fe-S protein 5	ENSRNOP00000037699	5	238	0.03	-1.50
22	Microtubule-associated protein Tau	ENSRNOP00000047817	3	1156	0.025	-1.60
23	NADH dehydrogenase (ubiquinone) 1 alpha subcomplex 5	ENSRNOP00000008325	5	526	0.034	-1.60
24	NADH dehydrogenase (ubiquinone) Fe-S protein 8	ENSRNOP00000023526	5	297	0.003	-1.70
25	ATP synthase, H+ transporting, mitochondrial Fo complex, subunit d	ENSRNOP00000004836	8	337	0.035	-1.80
26	Ubiquinol-cytochrome C reductase, complex III, subunit VI	ENSRNOP00000033706	8	258	0.046	-1.80
27	Calmodulin	ENSRNOP00000005755	13	731	2.85E-02	-1.90
28	Inositol 1,4,5-trisphosphate receptor type 1	ENSRNOP00000009288	5	230	0.003	-1.90
29	NADH dehydrogenase (ubiquinone) Fe-S protein 4	ENSRNOP00000015217	5	265	0.011	-2.20
30	NADH dehydrogenase (ubiquinone) flavoprotein 2	ENSRNOP00000016965	5	341	0.008	-2.60
31	protein phosphatase 3 (formerly 2B), regulatory subunit B, alpha isoform	ENSRNOP00000037143	9	626	0.004	-3.00
32	Cytochrome c oxidase subunit VIb polypeptide 1	ENSRNOP00000030997	2	109	0.011	-3.10
33	Disintegrin and metalloproteinase domain-containing protein 17	ENSRNOP00000010648	2	57	0.018	-3.30
34	synuclein, alpha (non A4 component of amyloid precursor)	ENSRNOP00000030609	5	390	0.002	-3.90

Regulated proteins of the AD pathway in the PHC ranked by fold change (relation of relative protein abundances between control and animals post SE). There are no proteins regulated at 8 weeks post SE.

[a] Accession number of identified proteins as given in Ensembl protein database (http://www.ensembl.org)

Thresholds were set at: [b] Peptides used for quantification > 2, [c] Confidence score > 30 and [d] p-value < 0.05

S: Surfaceome; N: nucleus; C: cytoplasm.

Table 2
Continuation

#	Gene Symbol	Accession codea	Peptides used for quantificationb	Confidence Scorec	Anova (p)d	Fold change
		8 weeks post SE				
1	Apolipoprotein E	ENSRNOP00000050968	11	731	0.0003	4.80
2	Amyloid beta (A4) precursor protein	ENSRNOP00000040243	2	101	9.00E-05	1.90
3	Hydroxysteroid (17-beta) dehydrogenase 10	ENSRNOP00000043608	7	440	0.001	1.60
4	nitric oxide synthase 1, neuronal	ENSRNOP00000001493	4	159	9.80E-05	1.60
5	Prolow-density lipoprotein receptor-related protein 1	ENSRNOP00000034210	18	687	2.29E-05	1.60
6	ubiquinol-cytochrome c reductase hinge protein	ENSRNOP00000016751	2	156	0.01376	1.50
7	ATP synthase, H+ transporting, mitochondrial F1 complex, beta polypeptide	ENSRNOP00000003965	42	2777	0.007	1.40
8	NADH Dehydrogenase (Ubiquinone) 1 Alpha Subcomplex, 3	ENSRNOP00000019141	3	75	0.033	1.40
9	NADH dehydrogenase (ubiquinone) Fe-S protein 3	ENSRNOP00000012425	8	457	0.00011	1.40
10	ubiquinol-cytochrome c reductase, complex III subunit VII	ENSRNOP00000065074	2	92	0.02183	1.40
11	Cytochrome c oxidase subunit IV isoform 1	ENSRNOP00000024033	9	391	0.044	1.30
12	NADH dehydrogenase (ubiquinone) Fe-S protein 1	ENSRNOP00000015851	34	2064	0.00107	1.30
13	NADH dehydrogenase (ubiquinone) Fe-S protein 2	ENSRNOP00000055224	8	494	0.00044	1.30
14	ubiquinol cytochrome c reductase core protein 2	ENSRNOP00000021514	21	1217	0.00539	1.30
15	ATP synthase, H+ transporting, mitochondrial F1 complex, alpha subunit 1, cardiac muscle	ENSRNOP00000022892	29	1956	0.001	1.20
16	Guanine nucleotide binding protein (G protein), q polypeptide	ENSRNOP00000019174	7	583	0.0023	1.20

Regulated proteins of the AD pathway in the PHC ranked by fold change (relation of relative protein abundances between control and animals post SE). There are no proteins regulated at 8 weeks post SE.

[a] Accession number of identified proteins as given in Ensembl protein database (http://www.ensembl.org)

Thresholds were set at: [b] Peptides used for quantification > 2, [c] Confidence score > 30 and [d] p-value < 0.05

S: Surfaceome; N: nucleus; C: cytoplasm.

Table 2
Continuation

#	Gene Symbol	Accession codea	Peptides used for quantificationb	Confidence Scorec	Anova (p)d	Fold change
17	Mitogen activated protein kinase 3	ENSRNOP00000026627	4	713	0.006	1.20
18	NADH dehydrogenase (ubiquinone) 1, subcomplex unknown, 2	ENSRNOP00000016509	3	139	0.03654	1.20
19	succinate dehydrogenase complex, subunit A, flavoprotein (Fp)	ENSRNOP00000018336	19	1331	0.00094	1.20
20	ubiquinol-cytochrome c reductase core protein I	ENSRNOP00000044696	16	1095	0.01982	1.20
21	ATPase, Ca++ transporting, cardiac muscle, slow twitch 2 (Atp2a2), transcript variant 2, mRNA	ENSRNOP00000001738	20	1891	0.046	1.10
22	protein phosphatase 3, catalytic subunit, beta isozyme	ENSRNOP00000010476	8	817	0.03945	1.10
23	ATP synthase, H+ transporting, mitochondrial Fo complex, subunit B1 (Atp5f1), mRNA	ENSRNOP00000021920	10	418	0.008	-1.10
24	Cytochrome c oxidase, subunit VIa, polypeptide 1	ENSRNOP00000001545	2	164	0.049	-1.30
25	Cytochrome c, somatic	ENSRNOP00000014058	6	328	0.027	-1.40
26	NADH dehydrogenase (ubiquinone) 1 alpha subcomplex, 6 (B14)	ENSRNOP00000011484	3	168	0.00101	-1.40
27	NADH dehydrogenase (ubiquinone) flavoprotein 3	ENSRNOP00000001564	12	981	0.04571	-1.50
28	ATP synthase, H+ transporting, mitochondrial F0 complex, subunit d	ENSRNOP00000004836	5	356	0.04	-1.90
29	ATP synthase, H+ transporting, mitochondrial F1 complex, epsilon subunit	ENSRNOP00000067815	2	74	0.0003	-2.30

Regulated proteins of the AD pathway in the PHC ranked by fold change (relation of relative protein abundances between control and animals post SE). There are no proteins regulated at 8 weeks post SE.

[a] Accession number of identified proteins as given in Ensembl protein database (http://www.ensembl.org)

Thresholds were set at: [b] Peptides used for quantification > 2, [c] Confidence score > 30 and [d] p-value < 0.05

S: Surfaceome; N: nucleus; C: cytoplasm.

Legends to figures

Figure 1

Proteins functionally linked with AD during the time course of epileptogenesis.

A) KEGG AD pathway at ten dpSE in the PHC. Regulated key proteins (as indicated by DAVID) are marked with an asterisk. Note the pronounced regulation of mitochondrial proteins, proteins associated with Aβ processing, deposition and plaque formation, the regulation of the microtubule-associated protein Tau and the regulation of proteins associated with calcium signaling.

B-D) The Venn diagrams illustrate the overlap of differentially expressed proteins of hippocampal and parahippocampal cortex tissues with the AD reference proteins at two dpSE, ten dpSE and eight wpSE.

Figure 2

Expression analysis of proteins linked with mitochondrial dysfunction (A-G) and calcium signaling (H-M) during the time course of epileptogenesis in the HC and PHC.

A, B: Expression patterns of identified mitochondrial proteins in the HC (**A**) and PHC (**B**) giving a trend of the regulation direction at the three analyzed time points (up-regulation: increased expression following SE; down-regulation: reduced expression following SE). **C-G**: Heat maps illustrating expression of all differentially expressed mitochondrial proteins in the HC (**C, D**) and PHC (**E-G**) as well as expression of proteins linked with calcium signaling in the HC (**H-J**) and PHC (**K-M**). Columns show individual log2 transformed protein abundances of regulated mitochondrial proteins. Cell notes (**H-M**) represent the absolute non-log transformed individual fold change. Lines are hierarchically clustered and correspond to single proteins. < 1/green = down-regulated in SE compared to controls, >1/red = up-regulated in SE compared to controls. 2 dpSE = two days post SE, 10 dpSE = ten days post SE, 8 wpSE = eight weeks post SE.

Figure 3

Heat maps illustrating expression of proteins linked with microtubule-associated protein Tau, proteins associated with Aβ processing, deposition, plaque formation, and Aβ-

associated pathology, proteins associated with neurodegeneration and other proteins during the time course of epileptogenesis in the HC (A-C) and the PHC (D-F).

Columns show individual log2 transformed protein abundances of quantified proteins. Lines are hierarchically clustered and correspond to single proteins with cell notes representing their absolute non-log transformed individual fold change. Differentially expressed proteins are marked with an asterisk. < 1/green = down-regulated in SE compared to controls, >1/red = up-regulated in SE compared to controls. 2 dpSE = two days post SE, 10 dpSE = ten days post SE, 8 wpSE = eight weeks post SE.

Expression analysis by individual fold changes (protein abundance of control and animals post SE divided by the protein abundance by the mean abundance of the respective control group) of selected proteins ApoE, Mapt-204 and Snca during the time course of epileptogenesis in the HC (**G**) and PHC (**H**).

I-J: Immunohistochemical validation of Tau protein expression in the PHC ten dpSE. **C:** Tau expression tended to be reduced in the PHC but slightly did not reach significance (p=0.057). Immunohistochemical staining of Tau and the neuronal marker NeuN is shown in the PHC ten dpSE in an electrode-implanted control animal and in a SE animal (**J**). Tau-immunoreactivity in dark blue was detected in the cytoplasm and in the cell processes. NeuN-positive cells appear with a pink nucleus. All neurons express Tau. Double labeled Tau/NeuN-cells are marked with white arrows. Black arrows highlight Tau-positive cells with a glia-like structure. Scale bar: 50 µm.

Figure 4

Immunohistochemical validation of ApoE protein expression in the HC and PHC.

A, B Hippocampal ApoE quantification ten dpSE in control and epileptic animals. **C** Representative ApoE immunohistochemistry ten dpSE in the CA3 region in control (left panel) and SE animals (right panel). **D, E** Parahippocampal ApoE quantification at Bregma – 3.14 for all three analyzed time points and **F** representative ApoE immunohistochemistry two dpSE. All data are given as mean ± SEM, * $p < 0.05$. Scale bars: 100 µm.

Annex

SI Fig. 1

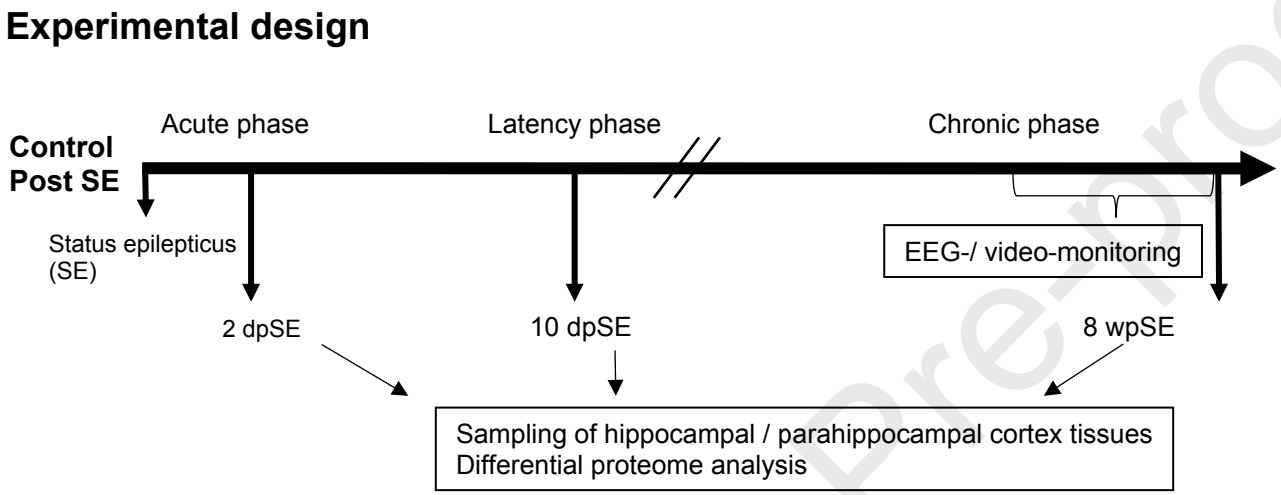

Supplementary Table 1

Regulated mitochondrial proteins functionally linked with AD in the HC and their individual fold changes.

Protein	Control 1	Control 2	Control 3	Control 4	Control 5	SE 1	SE 2	SE 3	SE 4	SE 5
					2 days post SE					
Atp5a1	1.03	0.99	0.92	1.04	1.02	1.16	1.07	1.25	1.24	1.21
Atp5b	1.08	0.94	0.93	1.06	0.99	1.13	1.39	1.38	1.27	1.10
Atp5c1	1.03	0.95	0.96	1.00	1.06	1.23	1.27	1.21	1.32	1.39
Cox4i1	0.77	0.92	1.02	1.06	1.24	1.10	1.34	1.18	1.22	1.23
Cyc1	1.04	0.95	0.98	0.98	1.04	1.12	1.17	1.09	1.12	1.05
Ndufa6	0.92	0.92	0.94	1.03	1.19	0.72	0.93	0.67	0.86	0.85
Ndufb5	0.91	0.91	1.03	1.07	1.08	1.21	1.48	1.50	1.28	1.52
Ndufb7	0.95	0.89	1.04	1.01	1.11	1.30	1.29	1.05	1.34	1.33
Ndufb8	0.88	0.95	1.00	1.15	1.01	1.02	1.69	1.57	1.25	1.51
Sdha	0.96	0.96	1.06	1.03	0.99	1.00	1.13	1.23	1.05	1.14
Sdhb	1.21	0.88	1.04	0.90	0.97	1.32	1.28	1.11	1.32	1.19
Sdhc	0.95	1.71	0.97	0.66	0.70	1.53	1.43	1.85	1.32	3.87
Uqcrc2	0.96	0.98	0.99	1.02	1.06	1.04	1.14	1.24	1.15	1.18
Uqcrfs1	1.12	0.92	0.97	0.99	0.99	1.55	1.37	1.20	1.46	1.40
					10 days post SE					
Gapdh	1.11	0.92	1.03	1.01	0.92	0.71	0.78	0.83	0.88	0.76

An individual fold change (protein abundance of control and animals post SE divided by the mean abundance of the respective control group) < 1 refers to a down-regulated protein.
An individual fold change > 1 refers to an up-regulated protein. There are no proteins regulated at 8 weeks post SE.

Supplementary Table 2

Regulated mitochondrial proteins functionally linked with AD in the PHC and their individual fold changes.

Protein	Control 1	Control 2	Control 3	Control 4	Control 5	SE 1	SE 2	SE 3	SE 4	SE 5
					2 days post SE					
Atp5f1	1.10	1.04	0.92	1.04	0.90	1.22	1.24	1.28	1.31	1.24
Cox6a1	1.15	0.61	1.67	0.69	0.88	1.60	2.04	1.26	1.40	2.06
Cox6c	1.10	1.01	0.97	0.95	0.96	1.11	1.00	1.11	1.25	1.21
Cox7b	1.13	0.87	1.26	0.81	0.92	1.38	0.97	1.32	2.03	2.30
Cyc1	0.99	0.98	0.99	1.04	0.99	1.16	1.12	1.07	1.31	1.40
Ndufa6	1.27	0.83	0.99	0.97	0.95	1.76	1.21	1.40	1.46	2.11
Ndufb4	1.00	0.92	1.01	1.05	1.02	1.13	1.07	1.14	1.24	1.18
Ndufs7	1.00	0.98	1.08	1.01	0.93	1.12	1.08	1.10	1.21	1.18
Sdhd	1.51	1.41	0.90	0.71	0.47	1.67	1.78	1.78	1.80	1.49
Uqcrc1	1.04	0.97	1.09	0.96	0.94	1.22	1.20	1.19	1.33	1.52
Uqcrc2	1.00	1.04	0.96	1.07	0.93	1.06	1.11	1.13	1.26	1.17
					10 days post SE					
Atp5f1	1.13	1.00	0.88	0.99	0.99	1.34	1.26	1.20	1.12	1.10
Atp5h	1.41	0.95	0.90	0.72	1.02	0.56	0.40	0.25	1.18	0.41
Atp5o	1.30	0.76	0.96	1.18	0.81	0.74	0.65	0.63	0.72	0.55
Cox6b1	1.72	0.71	0.47	0.99	1.11	0.34	0.24	0.15	0.74	0.14
Cox7a2l	1.03	0.98	1.00	0.91	1.09	1.16	1.21	1.10	1.14	1.09
Cyc1	0.95	0.91	1.09	0.96	1.08	1.14	1.23	1.12	1.21	1.29
Gapdh	1.10	1.02	1.04	0.94	0.91	0.82	0.88	0.71	0.87	0.71
Hsd17b10	0.99	0.89	1.02	1.13	0.98	1.31	1.33	1.35	1.22	1.06
Ndufa5	1.14	0.73	0.84	1.03	1.27	0.66	0.43	0.47	1.03	0.63
Ndufa6	0.98	0.79	0.85	1.12	1.25	1.27	1.16	1.16	1.43	1.53
Ndufc2	1.09	0.88	0.83	1.20	1.00	2.24	1.92	1.93	1.06	1.24
Ndufs3	0.86	0.86	1.07	1.10	1.10	1.34	1.30	1.26	1.16	1.29
Ndufs4	1.27	1.13	0.98	0.59	1.03	0.44	0.35	0.22	0.91	0.32

An individual fold change (protein abundance of control and animals post SE divided by the mean abundance of the respective control group) < 1 refers to a down-regulated protein.
An individual fold change > 1 refers to an up-regulated protein.

Supplementary Table 2

Continuation

Regulated mitochondrial proteins functionally linked with AD in the PHC and their individual fold changes.

Protein	Control 1	Control 2	Control 3	Control 4	Control 5	SE 1	SE 2	SE 3	SE 4	SE 5
					10 days post SE					
Ndufs5	1.13	1.07	1.08	0.88	0.85	0.93	0.62	0.43	0.90	0.51
Ndufs8	1.01	1.01	1.04	0.97	0.97	0.67	0.46	0.46	0.90	0.51
Ndufv1	1.11	0.97	1.07	0.99	0.86	0.95	0.87	0.80	0.91	0.67
Ndufv2	1.71	0.92	0.74	0.75	0.88	0.29	0.21	0.20	0.91	0.30
Sdhb	1.03	0.92	0.95	1.17	0.94	0.81	0.82	0.73	0.91	0.95
Uqcrb	1.33	0.76	0.80	0.96	1.14	0.57	0.39	0.25	1.32	0.24
Uqcrc1	0.95	0.92	1.07	1.01	1.06	1.24	1.25	1.29	1.21	1.02
Uqcrc2	1.03	0.96	1.02	1.04	0.95	1.30	1.41	1.21	1.10	1.26
Uqcrq	1.05	0.82	0.86	1.24	1.03	1.16	1.39	1.23	1.03	1.58
					8 weeks post SE					
Atp5a1	0.97	0.93	0.96	1.04	1.11	1.18	1.16	1.22	1.26	1.37
Atp5b	1.05	0.84	0.84	0.99	1.28	1.38	1.27	1.20	1.49	1.56
Atp5e	1.09	0.92	0.89	0.82	1.29	0.38	0.36	0.67	0.38	0.39
Atp5f1	0.96	0.99	0.95	1.05	1.05	0.86	0.83	0.89	0.83	0.98
Atp5h	1.30	0.84	0.83	0.56	1.47	0.42	0.29	1.14	0.41	0.37
Cox4i1	1.07	1.05	1.22	0.91	0.75	1.25	1.09	1.83	1.25	1.28
Cox6a1	1.18	0.96	1.10	0.86	0.90	0.87	0.59	1.06	0.67	0.55
Cycs	1.21	0.88	0.82	0.87	1.22	0.79	0.60	0.83	0.78	0.48
Hsd17b10	0.88	0.96	0.98	1.04	1.14	1.28	1.49	1.32	1.71	1.95
Ndufa3	1.03	0.61	1.10	1.16	1.11	1.60	1.16	1.59	1.16	1.61
Ndufa6	0.97	0.91	1.10	1.08	0.94	0.75	0.62	0.86	0.64	0.66
Ndufc2	1.12	0.89	1.12	1.02	0.85	1.15	1.16	1.49	1.06	1.30
Ndufs1	1.04	0.94	1.13	0.99	0.91	1.34	1.17	1.41	1.21	1.34

An individual fold change (protein abundance of control and animals post SE divided by the mean abundance of the respective control group) < 1 refers to a down-regulated protein.
An individual fold change > 1 refers to an up-regulated protein.

Supplementary Table 2

Continuation

Regulated mitochondrial proteins functionally linked with AD in the PHC and their individual fold changes.

Protein	Control 1	Control 2	Control 3	Control 4	Control 5	SE 1	SE 2	SE 3	SE 4	SE 5
					8 weeks post SE					
Ndufs2	1.03	0.92	1.07	0.96	1.03	1.25	1.20	1.46	1.24	1.39
Ndufs3	1.02	0.90	1.08	1.02	0.97	1.30	1.26	1.53	1.38	1.43
Ndufv3	1.53	0.63	0.83	1.00	1.01	0.68	0.48	0.71	0.76	0.65
Sdha	0.97	1.02	0.99	1.01	1.01	1.19	1.18	1.07	1.10	1.24
Uqcrc1	1.00	0.96	1.07	0.95	1.01	1.21	1.04	1.57	1.19	1.17
Uqcrc2	0.96	0.91	1.03	1.04	1.06	1.23	1.06	1.53	1.32	1.50
Uqcrh	1.20	1.28	0.71	0.92	0.89	1.64	1.44	1.20	1.33	1.74
Uqcrq	0.84	0.91	1.01	1.34	0.91	1.39	1.40	1.01	1.51	1.79

An individual fold change (protein abundance of control and animals post SE divided by the mean abundance of the respective control group) < 1 refers to a down-regulated protein.
An individual fold change > 1 refers to an up-regulated protein.

Highlights

- Proteins linked with Alzheimer pathogenesis are dysregulated during epileptogenesis.
- Proteins affecting mitochondrial function and calcium homeostasis are dysregulated.
- Prominent regulation of proteins involved in Aβ processing and regulation.
- Development and manifestation of both diseases share molecular alterations.